

Residual Tangent Kernels

Etai Littwin¹ Lior Wolf^{1,2}

Abstract

A recent body of work has focused on the theoretical study of neural networks at the regime of large width. Specifically, it was shown that training infinitely-wide and properly scaled vanilla ReLU networks using the L2 loss is equivalent to kernel regression using the Neural Tangent Kernel, which is independent of the initialization instance, and remains constant during training. In this work, we derive the form of the limiting kernel for architectures incorporating bypass connections, namely residual networks (ResNets), as well as to densely connected networks (DenseNets). In addition, we derive finite width corrections for both cases. Our analysis reveals that deep practical residual architectures might operate much closer to the “kernel” regime than their vanilla counterparts: while in networks that do not use skip connections, convergence to the limiting kernels requires one to fix depth while increasing the layers’ width, in both ResNets and DenseNets, convergence to the limiting kernel may occur for infinite deep and wide networks, provided proper initialization.

1. Introduction

Understanding the effect of different architectures on the ability to train deep networks has long been a major topic of research. A popular playing ground for studying the forward and backward propagation of signals at the point of initialization, is the “infinite width” regime (Arora et al., 2020; Sirignano & Spiliopoulos, 2019; Schoenholz et al., 2017; Yang & Schoenholz, 2017). In this regime and for some architectures, the central limit theorem applies when the weights are sampled i.i.d, guaranteeing the convergence of pre-activations to Gaussian Processes (GP), simplifying the analysis considerably (Lee et al., 2017). By viewing neural networks at their initialized state through the lens of GP’s, a link to kernel methods is revealed. Indeed, it has

¹Tel Aviv University ²Facebook AI Research. Correspondence to: Lior Wolf <wolf@cs.tau.ac.il, wolf@fb.com>.

been shown that under certain conditions, shallow training (where only the top layer is trained), is equivalent to kernel regression, where the kernel is defined by a GP (Arora et al., 2019).

While the analysis of initialized networks has traditionally been thought of as a first step towards understanding of the full training dynamics of neural networks, recent findings suggest a much stronger link between initialized networks, and their final convergent state post-training, especially for large width networks. While characterizing the full training dynamics of practically-sized networks remains an open problem, a certain limiting behavior was shown to emerge in large width networks, where perfect fitting of the training data using gradient descent is achieved with a minimal alteration of the weights compared to their initialized state. This notion is made precise by a recent paper on the Neural Tangent Kernel (NTK) (Jacot et al., 2018), in which it is shown that the training dynamics of fully connected networks trained with gradient descent can be characterized by a kernel, when the width of the network approaches infinity. In other words, the evolution through time of the function computed by the network follows the dynamics of kernel gradient descent.

Given a dataset $\{x\}_{i=1}^N$, let $f(x, W) \in \mathbb{R}$ denote the output of a fully connected feed forward network, with weights W for input x . The NTK is given by $K \in \mathbb{R}^{N \times N}$ such that:

$$K(x, x') = \mathbb{E}_W \left[\frac{\partial f(x)}{\partial W} \frac{\partial f(x')^\top}{\partial W} \right] := \mathbb{E}_W[\mathcal{G}(x, x')] \quad (1)$$

As the width of each layer approaches infinity, provided proper scaling and initialization of the weights, the expectation in Eq. 1 can be removed, and it holds that $\mathcal{G}_{i,j}$ converges in probability to the kernel function:

$$\lim_{\text{width} \rightarrow \infty} \mathcal{G}(x, x') \rightarrow K(x, x') \quad (2)$$

In the limit, minimizing the squared loss $\mathcal{L}(W)$ by gradient descent with an infinitely small learning rate is equivalent to kernel regression, with the evolution of the cost obeying the following dynamics:

$$\frac{\partial \mathcal{L}(W)}{\partial t} = \frac{\partial \mathcal{L}(W)}{\partial \mathbf{f}} K \frac{\partial \mathcal{L}(W)^\top}{\partial \mathbf{f}} \quad (3)$$

where $\mathbf{f} = [f(x_1, W) \dots f(x_N, W)]^\top \in \mathbb{R}^{N \times 1}$ denotes the vectorized form of the output on the entire training dataset.

From the positive definiteness of the limiting kernel K , convergence to zero training error when using gradient descent is then guaranteed.

While this view of neural network optimization does shed light on the empirical observations regarding the ease of optimization, the question of generalization remains elusive. Recently, empirical support has demonstrated the power of CNTK (convolutional neural tangent kernel) on practical datasets, demonstrating new state of the art results for kernel methods, surpassing other known kernels by a large margin (Arora et al., 2019; Yu et al., 2020). Although the performance gap compared with state of the art deep learning architectures remains non trivial, understanding the source of such a leap in performance compared with other kernel methods might shed new light on the inductive bias of neural networks, as explored in (Bietti & Mairal, 2019). It is, therefore, interesting to understand how far the training dynamics of practically sized architectures deviate from the “infinite width” regime. To that end, an important subtlety worth considering is the rate of convergence in Eq. 2 to the limit, and its dependence on other hyper parameters, such as depth.

This question has recently been addressed in the case of vanilla feed forward fully connected networks (Hanin & Nica, 2020), where it is shown that the variance of the diagonal entries of \mathcal{G} is exponential in the ratio between width and depth, and so convergence to the limiting kernel cannot happen when both are taken to infinity at the same rate. This important observation suggests that deep vanilla networks operate far from the “infinite width” regime.

Since the NTK and its convolutional counterpart were derived for vanilla feed forward architectures, it is natural to ask whether similar limiting kernels can be derived for additional, more prominent architectures. In this work, we explore the corresponding neural tangent kernel of residual architectures, namely ResNets (He et al., 2015a) and DenseNets (Huang et al., 2016). Furthermore, we rigorously derive finite width corrections for both architectures, revealing a fundamentally different relationship between width, depth and the NTK. Unlike vanilla architectures, when properly scaled, convergence to the limiting kernel is achieved when taking both the width and the depth of the architecture to infinity simultaneously. Our main contributions are:

- We formally draw correspondence between ResNets and DenseNets, to Gaussian processes in the infinite width limit, and rigorously derive the form of the corresponding NTK in this regime.
- We prove a forward-backward norm propagation duality for a wide family of ReLU architectures, and use it to derive bounds on the variance of the components of \mathcal{G} for finite sized networks. Specifically, we show that

for a properly initialized ResNets:

$$V(\mathcal{G}_{i,i}) \sim \mathcal{O}\left((mL)^2 \alpha^{2m} (\rho^2 - 1) \exp\left[L\alpha^m \rho\right]\right) \quad (4)$$

where m is the depth of each residual branch, L is the number of residual branches, $\rho = (1 + \frac{5}{n})^{\frac{m}{2}}$, n is the width, and α is an initialization constant multiplying normally distributed i.i.d weights. For a properly initialized DenseNets, our results show:

$$V(\mathcal{G}_{i,i}) \sim \mathcal{O}\left(\left(\exp\left[\frac{5}{n}\right] - 1\right) \log(L)^2\right) \quad (5)$$

Our results prove convergence to zero variance for ResNets when $\alpha \sim \frac{1}{L^{\frac{1}{m}}}$ (this initialization was also suggested in (Zhang et al., 2019) for training ResNets without batchnorm) when $n \rightarrow \infty$ regardless of depth. For DenseNets, worst case convergence to fixed variance is guaranteed using the standard $\frac{2}{fan-in}$ (He et al., 2015b) initialization, even when $n \sim \log(L)^2$. Both of these results are in stark contrast to the vanilla fully connected case, where the variance is exponential in $\frac{L}{n}$ (Hanin & Nica, 2020).

2. Related Work

The study of infinitely wide neural networks has been in the forefront of theoretical deep learning research in the last few years. A major line of work has been focused on the mean field approach, where the propagation of signals in random networks are analyzed in the regime of infinite width (Yang & Schoenholz, 2017; Schoenholz et al., 2017; Xiao et al., 2018)). In that case, the pre-activations in any layer are approximated by a Gaussian distribution with moments depending on the specific layer and initialization parameters. Depth scales that limit the maximum depth for which information can propagate can then be derived for different architectures and initialization. For standard fully connected feed forward models, for example, exponential collapsing of the input geometry is observed in (Schoenholz et al., 2017). Mean field analysis of residual networks is presented in (Yang & Schoenholz, 2017), where it is shown that ResNets exhibit sub-exponential, or even polynomial dynamics. A more refined analysis presented in (Pennington et al., 2017), considers the full spectrum of the input output Jacobian of infinitely wide networks, given by:

$$J_{IO} = \frac{\partial y^L}{\partial x} \quad (6)$$

where y^L is the final layer of the network, and x is the input. Exploding or vanishing gradients are then prevented, by analyzing conditions that give rise to dynamical isometry, a state in which the squared eigenvalues of J_{IO} are all concentrated around 1. In (Pennington et al., 2017) it is shown

that fully connected ReLU networks are incapable of reaching dynamical isometry, as opposed to sigmoidal networks, while in (Pennington et al., 2018) it is shown that dynamical isometry is achieved in a universal manner for a variety of activation functions. More recently, the dynamics of training infinitely wide networks were precisely described with the introduction of the Neural Tangent Kernel (Jacot et al., 2018), and its convolutional counterpart (Yu et al., 2020). Finite width corrections to the NTK in the vanilla case were introduced in (Hanin & Nica, 2020). In general, finite width corrections to various statistical quantities have been presented in numerous previous articles (Hanin & Rolnick, 2018), (Hanin, 2018).

(Hanin & Rolnick, 2018) tackle two failure modes that are caused in finite size networks by exponential explosion or decay of the norm of intermediate layers. It is shown that for random fully connected vanilla ReLU networks, the variance of the squared norm of the activations exponentially increases, even when initializing with the $\frac{2}{\text{fan-in}}$ initialization. For ResNets, this failure mode can be overcome by correctly rescaling the residual branches. However, it is not clear how such a rescaling affects the back propagation of gradients.

(Hanin, 2018) explores the conditions at initialization that give rise to the exploding or vanishing gradient problem, by analyzing the individual entries of the input-output Jacobian. As far as we can ascertain, finite width correction analysis of parameter gradients in residual architectures, as required to observe \mathcal{G} and its relationship with the NTK , have yet to be rigorously explored.

3. Preliminaries And Notations

We make use of the following notations: $f(x, W) \in \mathbb{R}$ denotes the output of a neural network \mathcal{N} on input x , where we assume without loss of generality that $\|x\|^2 = 1$. The ReLU non-linearity is denoted by $\phi()$, and intermediate outputs are denoted $\{y^l(x)\}_{l=0}^L$, for a fixed input $x \in \mathbb{R}^d$. For simplicity, the dependence of the outputs on x is often made implicit $\{y^l\}_{l=0}^L$ when the specific input used to calculate the outputs can be inferred from context. y_i^l denotes the i 'th component of the vector y^l , and $n_1 \dots n_L$ denote the width of the corresponding layers, with d the length of the input vector. $\|\cdot\|^2$ is the squared Euclidean norm. We denote the weight matrix associated with layer l by W^l , with lower case letters $w_{i,j}^l$ denoting the individual components of W^l . Additional superscripts $W^{l,k}$ are used, when several weight matrices are associated with layer l . Weights appearing without any superscript W denote all the weights concatenated to a vector. Each model analyzed begins and ends with an affine layer (no non-linearity), such that $y^0 = \frac{1}{\sqrt{d}}W^{s\top}x$, and $f(x) = \frac{1}{\sqrt{n_L}}W^{f\top}y^L$, where

$W^s \in \mathbb{R}^{d \times n_0}$, $W^f \in \mathbb{R}^{n_L \times 1}$. Throughout the paper, we assume that the weights are sampled i.i.d from a normal distribution.

4. Multi pathway Nets as Gaussian Processes

In this section, we draw an equivalence between random multi-pathway networks, namely ResNets and DenseNets, drawn using i.i.d Gaussian priors over the weights, and Gaussian processes. As observed in (Lee et al., 2017), the pre-activations of a feed forward neural network tend to i.i.d Gaussian processes as the width of the hidden layers tend to infinity. The proof of this claim usually involves taking the width of individual layers to infinity in a sequential manner (with the notable exception of (Yang, 2019)), ensuring that the previous layer is governed by its limiting distribution before considering the current layer. This presents a technical difficulty when considering multi-pathway networks, when the width of different layers are tied. For instance, naive addition operations without any form of downsampling in ResNets imply constant width. To overcome this technicality, we construct models such that width variables are disentangled, in a way that allows us to calculate the limiting distributions when taking width parameters consecutively to infinity.

4.1. ResNets

Residual networks have reintroduced the concept of bypass connections, allowing the training of deep and narrow models with relative ease. A generic, constant width residual architecture, with residual branches of depth m takes the form:

$$\forall_{0 < l \leq L}, y^l = y^{l-1} + y^{l-1,m} \quad (7)$$

where:

$$y^{l-1,h} = \begin{cases} \sqrt{\frac{\alpha}{n}} W^{l,h\top} q^{l-1,h-1} & 1 < h \leq m \\ \sqrt{\frac{\alpha}{n}} W^{l,h\top} y^{l-1} & h = 1 \end{cases} \quad (8)$$

with $q^{l-1,h} = \sqrt{2}\phi(y^{l-1,h})$, and α is an initialization parameter (see Fig. 1 for an illustration).

We define the following disentangled width residual network:

$$\forall_{0 < l \leq L}, y^l = [y^{l-1}]_{n_l} + y^{l-1,m} \quad (9)$$

where $[y^{l-1}]_{n_l}$ denotes the first n_l components of y^{l-1} , and:

$$y^{l-1,h} = \begin{cases} \sqrt{\frac{\alpha}{n_{l-1,h-1}}} W^{l,h\top} q^{l-1,h-1} & 1 < h \leq m \\ \sqrt{\frac{\alpha}{n_{l-1}}} W^{l,h\top} y^{l-1} & h = 1 \end{cases} \quad (10)$$

where $\forall_{1 < h < m}$, $W^{l-1,h} \in \mathbb{R}^{n_{l-1,h-1} \times n_{l-1,h}}$, $W^{l-1,1} \in \mathbb{R}^{n_{l-1} \times n_{l-1,1}}$, $W^{l-1,m} \in \mathbb{R}^{n_{l-1,m-1} \times n_l}$ and $\forall_{l_1 < l_2}$, $n_{l_1} > n_{l_2}$. we may now take the width of the network sequentially to infinity. Recall that the first

layer in any model considered is a simple affine layer with i.i.d Gaussian weights. Since the inputs are fixed, the first layer y^0 is, therefore, trivially a zero mean Gaussian process with covariance:

$$\forall_{0 < j \leq n_0} \mathbb{E}[y^0(x)_j y^0(x')_j] = \Sigma^{0,0}(x, x') = \frac{x^\top x'}{d} \quad (11)$$

By taking n_0 to infinity with other width parameters fixed, the pre-activations $y^{0,1}$ are given by an infinite sum of i.i.d random variables, and hence by the multivariate central limit theorem, tend to a GP with covariance:

$$\begin{aligned} \forall_{0 < j \leq n_{0,1}} \mathbb{E}[y^{0,1}(x)_j y^{0,1}(x')_j] &= \\ \frac{1}{n_0} \mathbb{E} \left[\left(\sum_{i=1}^{n_0} y^0(x)_i w_{i,j}^{1,1} \right) \left(\sum_{i=1}^{n_0} y^0(x')_i w_{i,j}^{1,1} \right) \right] &= \alpha \Sigma^{0,0}(x, x') \end{aligned} \quad (12)$$

In addition, the components of $q^{0,1} = \sqrt{2}\phi(y^{0,1})$ are then also distributed i.i.d, with covariance $\alpha \Sigma^{0,1}(x, x')$ such that:

$$\Sigma^{0,1}(x, x') = 2 \mathbb{E}_{u,v \sim \mathcal{N}(0, \Sigma^{0,0})} [\phi(u)\phi(v)] \quad (13)$$

The above argument can be extended by induction to the subsequent layers of the residual branch. Taking $n_{0,1}$ to infinity, the outputs $y^{0,2}$ are given by infinite sums of i.i.d variables, and so by the multivariate central limit theorem, tends to centered GP with covariance $\alpha^2 \Sigma^{0,1}(x, x')$. We arrive at the following recursion for $h > 0$:

$$\mathbb{E}[q^{0,h}(x)_j q^{0,h}(x')_j] = \alpha^h \Sigma^{0,h}(x, x') \quad (14)$$

$$\mathbb{E}[y^{0,h}(x)_j y^{0,h}(x')_j] = \alpha^h \Sigma^{0,h-1}(x, x') \quad (15)$$

where:

$$\Sigma^{l,h}(x, x') = \begin{cases} 2 \mathbb{E}_{u,v \sim \mathcal{N}(0, \Sigma^{l,h-1})} [\phi(u)\phi(v)] & 0 < h \leq m \\ \Sigma^l(x, x') & h = 0 \end{cases} \quad (16)$$

Note that when y^0 and $y^{0,m}$ achieve their limiting distribution, they become independent, and so $y^1 = [y^0]_{n_1} + y^{0,m}$ is a centered GP with covariance:

$$\Sigma^1(x, x') = \Sigma^0(x, x') + \alpha^m \Sigma^{0,m}(x, x') \quad (17)$$

Repeating this process for deeper layers, we arrive at the following inductive formula for the covariances of intermediate outputs:

$$\Sigma^l(x, x') = \Sigma^{l-1}(x, x') + \alpha^m \Sigma^{l-1,m}(x, x') \quad (18)$$

4.2. DenseNets

DenseNets were recently introduced, demonstrating faster training, as well as improved performance on several popular datasets. The main architectural features introduced by DenseNets include the connection of each layer output to all subsequent layers, using concatenation operations instead of summation, such that the weights of layer l multiply the concatenation of the outputs $y^0 \dots y^{l-1}$, and is of the dimensions $W^l \in \mathbb{R}^{ln \times n}$. For our analysis, we break W^l into $l-1$ weight matrices $W^{l,1} \dots W^{l,l-1} \in \mathbb{R}^{n \times n}$, so that the output of layer l is given by:

$$\forall_{0 < l \leq L}, y^l = \frac{1}{\sqrt{nl}} \sum_{h=0}^{l-1} W^{l,h\top} q^h, \quad q^h = \sqrt{2}\phi(y^h) \quad (19)$$

(see Fig. 1 for an illustration).

In order to use similar arguments as in the ResNet case, we define the following varying width DenseNets with intermediate outputs:

$$\forall_{0 < l \leq L}, y^l = \frac{1}{\sqrt{n'_{l-1} l}} \sum_{h=0}^{l-1} W^{l,h\top} [q^h]_{n'_{l-1}} \quad (20)$$

here $W^{l,h} \in \mathbb{R}^{n'_{l-1} \times n_l}$ and $\forall_{l > h}, n'_{l-1} \leq n_h$. Similar to the ResNet case, the pre-activations of the first layer y^0 , given a fixed input, are centered i.i.d GP, with covariance $\Sigma^0(x, x') = \frac{x^\top x'}{d}$. The covariances of subsequent layers are given by:

$$\begin{aligned} \forall_{0 < l \leq L}, \mathbb{E}[y^l(x)_j y^l(x')_j] &= \\ = \frac{1}{n'_l l} \left(\sum_{h=0}^{l-1} W^{l,h\top} [q^h(x)]_{n'_l} \right) \left(\sum_{h=0}^{l-1} W^{l,h\top} [q^h(x')]_{n'_l} \right) &= \\ = \frac{\sum_{h=1}^l \Sigma^h(x, x')}{l} & \end{aligned} \quad (21)$$

where $\Sigma^l(x, x') = \mathbb{E}[q^l(x)_j q^l(x')_j]$. We now push the width variables to infinity consecutively $n_0, n'_0, n_1, n'_1, n_2, \dots, n_L \rightarrow \infty$. The key observation in the DenseNet case is that for $l > 0$, the pre-activations $y^l, l > 0$ do not reach the limiting distribution until n'_{l-1} is pushed to infinity. When $n'_{l-1} \rightarrow \infty$, y^l is composed of a sum of l independent Gaussian processes given by $\{W^{l,h\top} [q^h]_{n'_{l-1}}\}_{h=0}^{l-1}$, and is, therefore, a GP with covariance $\frac{\sum_{h=1}^l \Sigma^h(x, x')}{l}$. We arrive at the induction:

$$\Sigma^{l+1}(x, x') = 2 \mathbb{E}_{u,v \sim \mathcal{N}(0, \frac{\sum_{h=1}^l \Sigma^h(x, x')}{l})} [\phi(u)\phi(v)] \quad (22)$$

4.3. Residual Tangent Kernels

Having formally drawn an equivalence between infinitely wide residual architectures, and Gaussian processes at initialization, the connection to kernel methods can now be

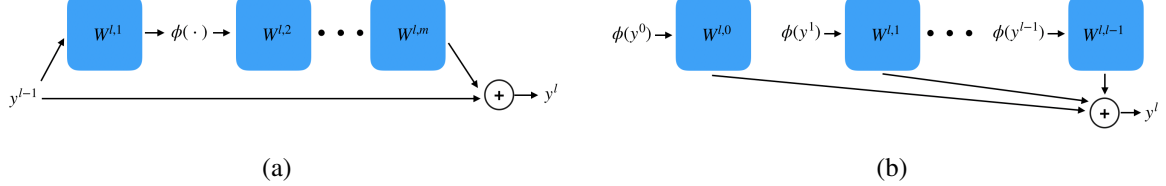


Figure 1. An illustration of (a) ResNet and (b) DenseNet as given in Eq. 8 and Eq. 19 (absent scaling coefficients).

made rigorous. As stated in (Arora et al., 2019), the equivalent of bayesian inferencing using a GP kernel is training only the top layer of the infinitely wide model. As such, it does not give special insight into the full training dynamics of neural networks. The full training dynamics, in the infinite width regime, are better addressed by the analysis of the corresponding neural tangent kernel. We devote the following theorems to derive the NTK for ResNets and DenseNets, where we assume, for the sake of derivation clarity, that the weights W^s, W^f do not participate in the optimization.

Theorem 1. *At initialization, for a depth L ResNet, with output $f(x)$ as the width $n_0, n_0, \dots, n_{L-1}, \dots, n_L' \rightarrow \infty$ consecutively, it holds that $\mathcal{G}(x, x')$ converges (in law) to $K_L^R(x, x')$ such that:*

$$K_L^R = K_{L-1}^R \left(\alpha^m \prod_{h=1}^{m-1} \dot{\Sigma}^{L-1, h} + 1 \right) + \alpha^m \sum_{h=1}^m \left(\Sigma^{L, h-1} \prod_{h'=h}^{m-1} \dot{\Sigma}^{L, h'} \right) \quad (23)$$

where $K_1^R = \alpha^m \sum_{h=1}^m \left(\Sigma^{0, h-1} \prod_{h'=h}^{m-1} \dot{\Sigma}^{0, h'} \right)$, $\{\Sigma^{l, h}\}$ are defined in Eq. 16, and:

$$\dot{\Sigma}^{l, h+1}(x, x') = 2 \mathbb{E}_{u, v \sim \mathcal{N}(0, \Sigma^{l, h})} [\dot{\phi}(u) \dot{\phi}(v)] \quad (24)$$

where $\dot{\phi}(u)$ denotes the derivative of ϕ by u .

Moreover, the diagonal components of K^R are given by:

$$K_L^R(x, x) = mL\alpha^m \left(1 + \alpha^m \right)^{L-1} \quad (25)$$

The following theorem states our result for DenseNets.

Theorem 2. *At initialization, for a depth L DenseNet, with output $f(x)$ as the width $n_0, n_0, \dots, n_L \rightarrow \infty$ consecutively, it holds that $\mathcal{G}(x, x')$ converges (in law) to $K_L^D(x, x')$, such that:*

$$K_L^D = \sum_{l=1}^L \frac{\sum_{h=0}^{l-1} \Sigma^h}{l} m^{l+1, l} \quad (26)$$

where $\{\Sigma^l\}$ are defined in Eq. 22, $m^{l+1, l}$ is defined recur-

sively:

$$m^{l, h} = \begin{cases} \frac{\dot{\Sigma}^h}{l} m^{l+1, l} + m^{l+1, h} & 0 < l < L \\ \frac{\dot{\Sigma}^h}{L} & l = L \\ 1 & \text{else} \end{cases} \quad (27)$$

and:

$$\dot{\Sigma}^{l+1}(x, x') = 2 \mathbb{E}_{u, v \sim \mathcal{N}(0, \frac{\sum_{h=1}^l \Sigma^h(x, x')}{l})} [\dot{\phi}(u) \dot{\phi}(v)] \quad (28)$$

Moreover, the diagonal components of K_L^D are given by:

$$K_L^D(x, x) = \sum_{l=1}^L \frac{1}{l+1} \quad (29)$$

We employed Monte Carlo simulations in order to verify the results of Theorems 1 and 2, as illustrated in Fig. 2. There is an excellent match between the simulations and our derivations.

5. Finite Width Corrections

The NTK provides an elegant glimpse into the training dynamics of infinite width networks. In this regime, provided that the loss is well-behaved, gradient descent becomes kernel gradient descent in functional space with the fixed neural tangent kernel, where no features are learned.

In practice, zero training error is also achieved also for deep and narrow residual architectures. It is, therefore, worth investigating how close the actual training dynamics of modern architectures (which usually contain residual connections) to the training dynamics of infinitely wide networks.

Specifically, we relax the fixed kernel assumption with a smoothness assumption. A differentiable function $f(W) : \mathbb{R}^d \rightarrow \mathbb{R}$ is β -smooth, if its gradient is β -Lipschitz. That is, for any u, v it holds $\|\nabla f(u) - \nabla f(v)\| \leq \beta \|u - v\|$.

The following lemma gives a sufficient condition for gradient descent to converge to zero training error for β -smooth functions.

Lemma 1. *Given a β -smooth function $f(u) \in [0, 1]$, a learning rate $0 \leq \alpha < \frac{1}{\beta}$ and a constant $0 < c < 1$.*

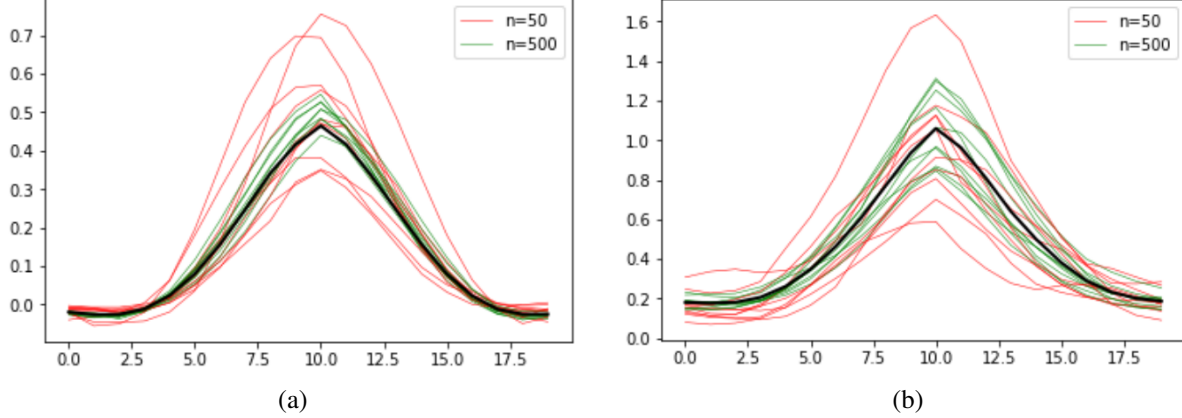


Figure 2. Plots of sampled $\mathcal{G}(x, x')$ for (a) a ResNet with $m=2$, and (b) a DenseNet, using two different widths (50,500). For the inputs, we used $x = [1, 0]$, and $x' = [\cos(\theta), \sin(\theta)]$ for 20 different values of θ . As expected, samples from wider networks (green lines) result in a lower variance compared with narrow networks (red lines). The black line corresponds to our theoretical expression for the NTK for both models, as given in Theorem 1 and Theorem 2.

Let $\{f(u_t)\}_{t=0}^\infty$ be the series of outputs given by applying gradient descent, such that $f(u_{t+1}) = f(u_t) - \alpha \nabla f(u_t)$. Assuming the following holds for any point u :

$$\|\nabla f(u)\| \geq \|\sqrt{2c\beta}f(u)\| \quad (30)$$

it then holds:

$$f(u_\infty) = 0 \quad (31)$$

When f is given by a neural network equipped with a strongly convex loss function, the condition on the gradient given in Eq. 30 can be guaranteed by the positive definiteness of \mathcal{G} . Similarly to Eq. 3 in the infinite case, the batch gradient squared norm in the finite case is given by:

$$\|\nabla \mathcal{L}(W)\|^2 = \frac{\partial \mathcal{L}}{\partial \mathbf{f}} \mathcal{G} \frac{\partial \mathcal{L}^\top}{\partial \mathbf{f}} \quad (32)$$

Considering a regression task, with input label pairs $\{x_i, y_i\}$ such that $f, y_i \in [0, 1]$, the functional gradient is lower bounded:

$$\|\frac{\partial \mathcal{L}}{\partial \mathbf{f}}(W)\| = 2\|\mathbf{f}(W) - \mathbf{y}\| \geq 2\mathcal{L}(W) \quad (33)$$

Plugging into Eq. 32, the condition on the gradient in Lemma 1 is, therefore, guaranteed when the minimum eigenvalue λ_{min} of \mathcal{G} is lower bounded by

$$\lambda_{min}(\mathcal{G}) \geq \frac{c\beta}{2}. \quad (34)$$

For infinitely wide networks, there exists a constant $0 < c < 1$ such that the condition in Eq. 34 is met, due to the positive definiteness of the NTK. For finite width networks, \mathcal{G} is random at initialization, and changes during training.

Moreover, the rate in which \mathcal{G} converges to its limit as width increases, depends on the depth of the network.

For vanilla feed forward models, the variance of the entries of \mathcal{G} is exponential in the ratio between depth to width (Hanin & Nica, 2020). Therefore, taking both parameters to infinity simultaneously, and at the same rate, maintains this variance, and \mathcal{G} does not converge to the NTK. However, as we show next, models employing residual connections, can display convergence to the NTK, even when depth increases at a pace faster than the width.

5.1. Forward-Backward Norm Propagation Duality

We aim to derive an expression for the first and second moments of the diagonal entries of \mathcal{G} at the point of initialization, given by the Jacobian squared norm evaluated on x_i :

$$\mathcal{G}(x, x) = \left\| \frac{\partial f(x)}{\partial W} \right\|^2 = \|J(x)\|^2 \quad (35)$$

In the following analysis, We assume the output f is computed using a single fixed sample x . In addition, we introduce the per layer Jacobian $J^k = \frac{\partial f}{\partial W^k}$ (here we use a single superscript k to identify weight matrices). To facilitate our derivation, we introduce a link between the propagation of the norm of the activations, and the norm of the Jacobian in different layers in random ReLU networks of finite width and depth. This link will then allow us to study the statistical properties of the Jacobian in general architectures incorporating residual connections and concatenations with relative ease. Specifically, we would like to establish a connection between the first and second moments of the squared norm of the output $(f)^2$, and those of the per layer Jacobian norm $\|J^k\|^2$. Using a path-based notation, the output f can be

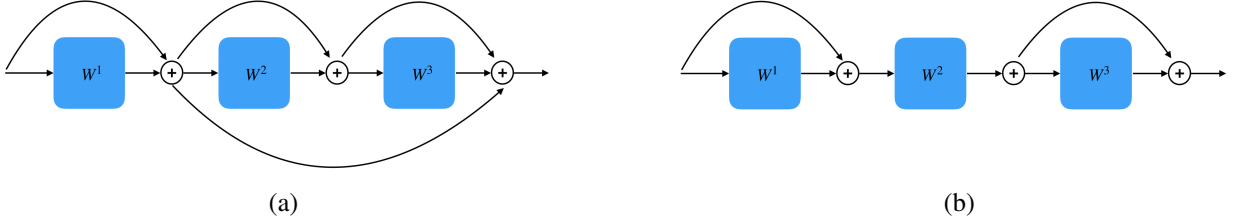


Figure 3. An illustration of Thm. 3. The activations of the network in (a) are completely different from those of the network in (b), in which all skip connections bypassing layer $k = 2$ are removed. However, the moments of the gradient norms at layer $k = 2$ are exactly the same in both (a) and (b).

decomposed to paths that go through weight matrix W^k , denoted by f^k , and paths that skip W^k , denoted by \hat{f}^k . Namely:

$$f = f^k + \hat{f}^k = \sum_{\gamma \in \gamma_k} c_\gamma z_\gamma \prod_{l=1}^{|\gamma|} w_{\gamma,l} + \sum_{\gamma \notin \gamma_k} c_\gamma z_\gamma \prod_{l=1}^{|\gamma|} w_{\gamma,l} \quad (36)$$

where the summation is over paths from input to output, indexed by γ , with $|\gamma|$ denoting the length of the path indexed by γ , and c_γ a scaling factor. In non-residual networks, we have $|\gamma| = L + 2$ (when considering the initial and final projections W^s, W^f) and \sum_γ sums over $d \prod_{l=0}^L n_l$ paths. The term $z_\gamma \prod_{l=1}^{|\gamma|} w_{\gamma,l}$ denotes the product of weights along path γ , multiplied by a binary variable $z_\gamma \in [0, 1]$, indicating whether path γ is active (i.e. all relevant activations along the specific path are on). The first summation $\sum_{\gamma \in \gamma_k}$ indicates summation over all possible paths that include a weight from layer k , while $\sum_{\gamma \notin \gamma_k}$ indicate summation over paths that do not include a weight from layer k . In all relevant architectures, the squared norm of the Jacobian entry $\|J_{i,j}^k\|^2$ is given by:

$$\|J_{i,j}^k\|^2 = \left\| \frac{\partial f^k}{\partial w_{i,j}^k} + \frac{\partial \hat{f}^k}{\partial w_{i,j}^k} \right\|^2 = \left\| \frac{\partial f^k}{\partial w_{i,j}^k} \right\|^2 \quad (37)$$

where the last transition stems from the fact that z_γ is binary, and $\frac{\partial z_\gamma}{\partial w_{i,j}^k} = 0$ everywhere except for a set of zero measure, where the derivative is ill-defined. The derivative of output with respect to weight $w_{i,j}^k$ is given by the sum of all paths γ that contain $w_{i,j}^k$ divided by $w_{i,j}^k$. In order to link J^k with f , we make the following definition:

Definition 1. *Reduced network: the outputs of a reduced network $f_{(k)}(W)$ denoted by $y_{(k)}^0 \dots y_{(k)}^L$ given input x are obtained by removing all connections bypassing weight W^k from the network $f(W)$.*

Note that for vanilla networks, it holds that $f_{(k)} = f^k = f$, and $\forall 0 \leq l \leq L$, $y_{(k)}^l = y^l$. The following Lemma links between the moments of $f_{(k)}$ and those of f^k :

Theorem 3. *For the architectures described in Sec. 4 (Eq. 8 and Eq. 19), using symmetrically distributed iid weights, with unit variance and finite fourth moment, the following holds at initialization for any non-negative even integer m :*

$$\forall_{W^k}, \mathbb{E} [\|f_{(k)}\|^m] = \mathbb{E} [\|f^k\|^m] \quad (38)$$

In the general case, the equality $f_{(k)} = f^k$ does not hold, since $f_{(k)}$ contains different activation patterns, induced by the removal of residual connections. However, Theorem 3 states that the moments of both are equal in the family of considered ReLU networks (see Fig. 3 for an illustration). The following theorem relates the moments of $\|J^k\|^2$ with those of $\|f_{(k)}\|$:

Theorem 4. *For the architectures described in Sec 4 (Eq. 8 and Eq. 19), using symmetrically distributed iid weights, with unit variance and finite fourth moment, the following holds at initialization:*

1. $\forall_{W^k}, \mathbb{E} [\|J^k\|^2] = E [\|f_{(k)}\|^2]$
2. $\forall_{W^k}, \frac{E [\|f_{(k)}\|^4]}{c_4} \leq \mathbb{E} [\|J^k\|^4] \leq E [\|f_{(k)}\|^4]$

where c_4 is the fourth moment of the weights. Thm. 4 indicates that we can compute the moments of the Jacobian norm of layer k , by computing the moments of the output of the reduced network $f_{(k)}$. Thm. 4 also allows us to derive an upper bound on the variance (V) of the full Jacobian squared norm:

$$V(\|J\|^2) \leq \left(\sum_k \sqrt{V(\|J^k\|^2)} \right)^2 \quad (39)$$

The following theorem states our results for ResNets:

Theorem 5. *For a constant width ResNet (Eq. 8), with $0 < \alpha < 1$ it holds that the variance of the diagonal elements of G behave asymptotically as*

$$V(\mathcal{G}_{i,i}) \sim \mathcal{O} \left((mL)^2 \alpha^{2m} (\rho^2 - 1) \exp \left[L \alpha^m \rho \right] \right) \quad (40)$$

where $\rho = (1 + \frac{5}{n})^{\frac{m}{2}}$

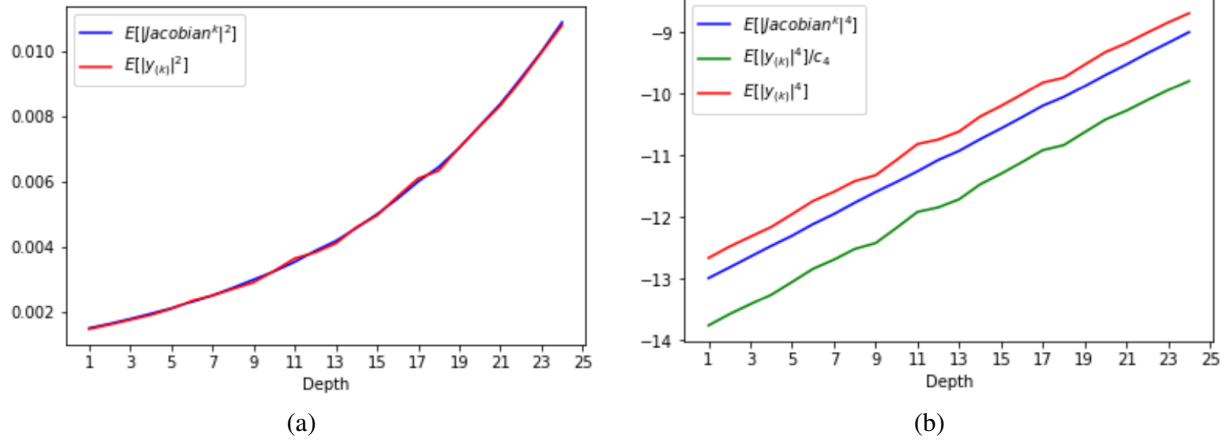


Figure 4. The (a) second (b) fourth moments, in log scale, of the per layer Jacobian norm $\|J^k\|$ and the squared norm of the output of the corresponding reduced architecture $\|f_{(k)}\|$, for a ResNet with $m = 2$, $\alpha = 0.3$ and varying depth. The results were obtained from the simulated results of 200 independent runs per depth, where the value for k is random for each depth. All networks were initialized using normal distributions $c_1 = 0$, $c_2 = 1$. As can be seen, the mean of both $\|J^k\|^2$ and $\|f_{(k)}\|^2$ closely match, while the fourth moment $\mathbb{E}[\|J^k\|^4]$ is upper and lower bounded, by the corresponding moments of the output, as predicted in Theorem 4.

From the result of Theorems 1 and 5, when fixing m , both the mean and variance of the diagonal components of \mathcal{G} are exponential in $\alpha^m L$. Setting $\alpha \sim \frac{1}{L^m}$, we are then guaranteed convergence to constant mean and zero variance when $n \rightarrow \infty$ regardless of depth, as shown in the next corollary:

Corollary 1. *For a constant width ResNet with constants $a > 0$, $\alpha = \frac{a}{L^m}$, it holds that:*

$$V(\mathcal{G}_{i,i}) \sim \mathcal{O}\left(\frac{1}{n}\right) \quad (41)$$

Note that the $\alpha \sim \frac{1}{L^m}$ initialization was also suggested in (Zhang et al., 2019), as a way to train ResNets without batchnorm. Our results, however, reveal a much stronger implication of this initialization, as it also bounds the fluctuations of the squared Jacobian norm, implying a closer relationship with the ‘‘kernel regime’’ when training deep ResNets.

The following theorem states our results for DenseNets:

Theorem 6. *For a constant width DenseNet (Eq. 19), it holds that:*

$$V(\mathcal{G}_{i,i}) \sim \mathcal{O}\left(\left(\exp\left[\frac{5}{n}\right] - 1\right) \log(L)^2\right) \quad (42)$$

For DenseNets, our results show exponential behavior in $\frac{5}{n}$, and squared logarithmic behavior in depth. Convergence to constant mean and zero variance is guaranteed when $n, L \rightarrow \infty$ at the same rate, as shown in the next corollary:

Corollary 2. *For a constant width DenseNet with constants*

$a > 0$, $n = aL$, it holds that:

$$V(\mathcal{G}_{i,i}) \sim \mathcal{O}\left(\frac{\log(L)^2}{L}\right) \quad (43)$$

The results of Theorem 2 and theorem 6 suggest an interesting observation unique to DenseNets. From Theorem 2, the mean of the diagonal components is logarithmic in depth $\mathcal{G}_{i,i} = \sum_{l=1}^L \frac{1}{l+1} \sim \log(L)$. The variance, however, is linear in the ratio $\frac{\log(L)^2}{n}$. That is, when $n, L \rightarrow \infty$ at the same rate, we have $\mathcal{G}_{i,i} \rightarrow K_{i,i}^D$. And so, dense connections both increase the expected squared norm of the Jacobian, while also decrease its variance as both the depth and width increase at similar rates.

Empirical support We employed Monte Carlo simulations in order to verify our theoretical findings in Theorems 4,5 and 6. This is shown in Figure 4 and 5.

6. Conclusions

The Neural Tangent Kernel has provided new insights into the training dynamics of wide neural networks, as well as their generalization properties, by linking them to kernel methods. In this work, we have formally specified the correspondence between residual architectures, and Gaussian Processes. We then used that link to derive the corresponding neural tangent kernel for the ResNet and DenseNet architectures. Using a duality principle between forward and backward norm propagation, we have derived finite width corrections for both architectures, and have shown convergence properties of deep models that are absent in the vanilla fully connected architectures. Our results shed new light on

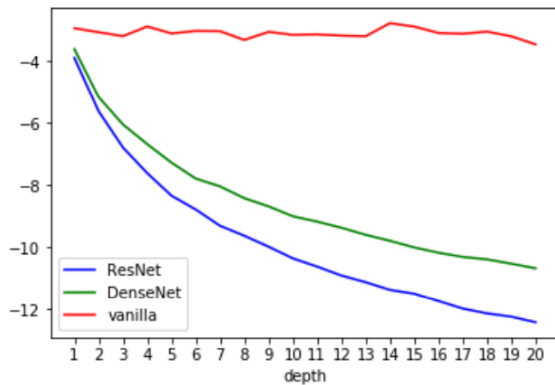


Figure 5. Variance in log scale of the full Jacobian squared norm for ResNet ($m = 2, \alpha = \frac{0.3}{\sqrt{L}}$), DenseNet and Vanilla network. For each architecture, the width is given by $n = cL$ where $c = 10$. The results were obtained from the simulated results of 200 independent runs per depth. As can be seen, the variance of the vanilla network remains constant due to the fixed ratio between depth and width, while ResNet and DenseNet exhibit convergence to the NTK as predicted by theorem 5 and theorem 6.

the effect of residual connections on the training dynamics, suggesting that models incorporating residual connections operate much closer to the so called “kernel regime” than vanilla architectures, even at increasing depths.

7. Acknowledgments

This project has received funding from the European Research Council (ERC) under the European Union’s Horizon 2020 research and innovation programme (grant ERC CoG 725974).

References

Arora, S., Du, S. S., Hu, W., Li, Z., Salakhutdinov, R., and Wang, R. On exact computation with an infinitely wide neural net. In *NeurIPS*, 2019.

Arora, S., Du, S. S., Li, Z., Salakhutdinov, R., Wang, R., and Yu, D. Harnessing the power of infinitely wide deep nets on small-data tasks. In *International Conference on Learning Representations*, 2020. URL <https://openreview.net/forum?id=rkl8sJBYvH>.

Bietti, A. and Mairal, J. On the Inductive Bias of Neural Tangent Kernels. In *NeurIPS 2019 - Thirty-third Conference on Neural Information Processing Systems*, pp. 1–24, Vancouver, Canada, December 2019. URL <https://hal.inria.fr/hal-02144221>.

Hanin, B. Which neural net architectures give rise to exploding and vanishing gradients? In Bengio, S., Wallach, H., Larochelle, H., Grauman, K., Cesa-Bianchi, N., and Garnett, R. (eds.), *Advances in Neural Information Processing Systems 31*, pp. 582–591. Curran Associates, Inc., 2018.

Hanin, B. and Nica, M. Finite depth and width corrections to the neural tangent kernel. In *International Conference on Learning Representations*, 2020. URL <https://openreview.net/forum?id=SJgndT4KwB>.

Hanin, B. and Rolnick, D. How to start training: The effect of initialization and architecture. In *NeurIPS*. 2018.

He, K., Zhang, X., Ren, S., and Sun, J. Deep residual learning for image recognition. *2016 IEEE Conference on Computer Vision and Pattern Recognition (CVPR)*, pp. 770–778, 2015a.

He, K. et al. Delving deep into rectifiers: Surpassing human-level performance on imagenet. In *ICCV*, 2015b.

Huang, G., Liu, Z., and Weinberger, K. Q. Densely connected convolutional networks. *2017 IEEE Conference on Computer Vision and Pattern Recognition (CVPR)*, pp. 2261–2269, 2016.

Jacot, A., Gabriel, F., and Hongler, C. Neural tangent kernel: Convergence and generalization in neural networks. In *Proceedings of the 32nd International Conference on Neural Information Processing Systems*, NIPS’18, pp. 8580–8589, Red Hook, NY, USA, 2018. Curran Associates Inc.

Lee, J., Bahri, Y., Novak, R., Schoenholz, S. S., Pennington, J., and Sohl-Dickstein, J. Deep neural networks as gaussian processes. *ArXiv*, abs/1711.00165, 2017.

Pennington, J., Schoenholz, S., and Ganguli, S. Resurrecting the sigmoid in deep learning through dynamical isometry: theory and practice. In Guyon, I., Luxburg, U. V., Bengio, S., Wallach, H., Fergus, R., Vishwanathan, S., and Garnett, R. (eds.), *Advances in Neural Information Processing Systems 30*, pp. 4785–4795. Curran Associates, Inc., 2017.

Pennington, J., Schoenholz, S. S., and Ganguli, S. The emergence of spectral universality in deep networks. In *AISTATS*, 2018.

Schoenholz, S., Gilmer, J., Ganguli, S., and Sohl-Dickstein, J. Deep information propagation. In *ICLR*, 11 2017.

Sirignano, J. and Spiliopoulos, K. Mean field analysis of deep neural networks. *arXiv preprint arXiv:1903.04440*, 2019.

Xiao, L., Bahri, Y., Sohl-Dickstein, J., Schoenholz, S., and Pennington, J. Dynamical isometry and a mean field theory of CNNs: How to train 10,000-layer vanilla convolutional neural networks. In Dy, J. and Krause, A. (eds.),

Proceedings of the 35th International Conference on Machine Learning, volume 80 of *Proceedings of Machine Learning Research*, pp. 5393–5402, Stockholmsmässan, Stockholm Sweden, 10–15 Jul 2018. PMLR.

Yang, G. Scaling limits of wide neural networks with weight sharing: Gaussian process behavior, gradient independence, and neural tangent kernel derivation, 02 2019.

Yang, G. and Schoenholz, S. S. Mean field residual networks: On the edge of chaos. In *Proceedings of the 31st International Conference on Neural Information Processing Systems*, NIPS’17, pp. 2865–2873, Red Hook, NY, USA, 2017. Curran Associates Inc. ISBN 9781510860964.

Yu, D., Wang, R., Li, Z., Hu, W., Salakhutdinov, R., Arora, S., and Du, S. S. Enhanced convolutional neural tangent kernels, 2020. URL <https://openreview.net/forum?id=BkgNqkHFPPr>.

Zhang, H., Dauphin, Y. N., and Ma, T. Residual learning without normalization via better initialization. In *International Conference on Learning Representations*, 2019. URL <https://openreview.net/forum?id=H1gsz30cKX>.

A. Proofs

A.1. Proof of Theorem 1

Proof. Recall that we need to compute $K_L(x, x')^R = \lim_{n_0 \dots n_L \rightarrow \infty} \sum_{l=1}^L \sum_{h=1}^m \left\langle \frac{\partial f(x, W)}{\partial W^{l,h}}, \frac{\partial f(x', W)}{\partial W^{l,h}} \right\rangle$. The derivative $\frac{\partial f(x, W)}{\partial W^{l,h}}$ can be written in a compact matrix form:

$$\forall 0 < l \leq L, \frac{\partial f(x, W)}{\partial W^{l,h}} = \begin{cases} \sqrt{\frac{(2\alpha)^{m-h}}{\prod_{h'=h-1}^{m-1} n_{l-1,h'}}} q^{l-1,h-1}(x) \left(C_h^l(x) A^{l+1}(x) \right)^\top & 1 < h \leq m \\ \sqrt{\frac{(2\alpha)^{m-h}}{\prod_{h'=h-1}^{m-1} n_{l-1,h'}}} y^{l-1}(x) \left(C_1^l(x) A^{l+1}(x) \right)^\top & h = 1 \end{cases} \quad (44)$$

where:

$$C_h^l(x) = \begin{cases} \prod_{h'=h}^{m-1} \left(\dot{Z}^{l,h'}(x) W^{l,h'+1} \right) & 1 < h < m \\ I & \text{else} \end{cases} \quad (45)$$

and:

$$A^l(x) = \begin{cases} \left(\alpha^{\frac{m}{2}} \sqrt{\frac{2^{m-1}}{\prod_{h'=0}^{m-1} n_{l-1,h'}}} W^{l,1} C_1^l(x) + I^l \right) A^{l+1}(x) & 0 < l \leq L \\ \frac{1}{\sqrt{n_L}} W^f & l = L \end{cases} \quad (46)$$

$Z^{l,h}$ is a diagonal matrix holding the binary activation variables of layer h in residual branch l in its diagonal, and $I^l = [I_{n_l}, \mathbf{0}_{n_{l-1}-n_l}]^\top \in \mathbb{R}^{n_{l-1} \times n_l}$ is a concatenation of an n_l dimensional identity matrix, and a zero matrix $\mathbf{0}_{n_{l-1}-n_l} \in \mathbb{R}^{n_l \times n_{l-1}-n_l}$. It follows:

$$\forall 1 < h \leq L \left\langle \frac{\partial f(x, W)}{\partial W^{l,h}}, \frac{\partial f(x', W)}{\partial W^{l,h}} \right\rangle \quad (47)$$

$$= \frac{(2\alpha)^{m-h+1}}{\prod_{h'=h-1}^{m-1} n_{l-1,h'}} \left\langle q^{l-1,h-1}(x) \left(C_h^l(x) A^{l+1}(x) \right)^\top, q^{l-1,h-1}(x') \left(C_h^l(x') A^{l+1}(x') \right)^\top \right\rangle \quad (48)$$

$$= \frac{(2\alpha)^{m-h+1}}{\prod_{h'=h-1}^{m-1} n_{l-1,h'}} \left\langle q^{l-1,h-1}(x), q^{l-1,h-1}(x') \right\rangle A^{l+1}(x)^\top C_h^l(x)^\top C_h^l(x') A^{l+1}(x') \quad (49)$$

Note that after taking the limits $n_0 \dots n_{l-1,h-1} \rightarrow \infty$, it holds that $\frac{1}{n_{l-1,h-1}} \left\langle q^{l-1,h-1}(x), q^{l-1,h-1}(x') \right\rangle \rightarrow \alpha^{h-1} \Sigma^{l-1,h-1}(x, x')$.

We are left with (after taking the limits $n_0 \dots n_{l-1,h-1} \rightarrow \infty$):

$$\lim_{n_0 \dots n_{l-1,h-1}} \left\langle \frac{\partial f(x, W)}{\partial W^{l,h}}, \frac{\partial f(x', W)}{\partial W^{l,h}} \right\rangle = \frac{2^{m-h+1} \alpha^m}{\prod_{h'=h}^{m-1} n_{l-1,h'}} \Sigma^{l-1,h-1}(x, x') A^{l+1}(x)^\top C_h^l(x)^\top C_h^l(x') A^{l+1}(x') \quad (50)$$

$$= \frac{2^{m-h+1} \alpha^m}{\prod_{h'=h}^{m-1} n_{l-1,h'}} \Sigma^{l-1,h-1}(x, x') A^{l+1}(x)^\top C_{h+1}^l(x) W^{l,h+1\top} \dot{Z}^{l,h}(x) \dot{Z}^{l,h}(x') W^{l,h+1} C_{h+1}^l(x') A^{l+1}(x') \quad (51)$$

Taking $n_{l-1,h} \rightarrow \infty$, it holds that $\frac{2}{n_{l-1,h}} W^{l,h+1\top} \dot{Z}^{l,h}(x) \dot{Z}^{l,h}(x') W^{l,h+1} \rightarrow \dot{\Sigma}^{l-1,h}(x, x') I$.

And so:

$$\begin{aligned} & \lim_{n_0 \dots n_{l-1,h} \rightarrow \infty} \left\langle \frac{\partial f(x, W)}{\partial W^{l,h}}, \frac{\partial f(x', W)}{\partial W^{l,h}} \right\rangle \\ &= \frac{(2^{m-h} \alpha^m)}{\prod_{h'=h+1}^{m-1} n_{l-1,h'}} \Sigma^{l-1,h-1}(x, x') \dot{\Sigma}^{l-1,h}(x, x') A^{l+1}(x)^\top C_{h+1}^l(x) C_{h+1}^l(x') A^{l+1}(x') \\ &= \alpha^m \Sigma^{l-1,h-1}(x, x') \prod_{h'=h}^{m-1} \dot{\Sigma}^{l-1,h'}(x, x') A^{l+1}(x)^\top A^{l+1}(x') \end{aligned} \quad (52)$$

It then follows:

$$\langle A^{l+1}(x), A^{l+1}(x') \rangle = A^{l+2}(x)^\top \left(\alpha^{\frac{m}{2}} \sqrt{\frac{2^{m-1}}{\prod_{h'=0}^{m-1} n_{l,h'}}} W^{l+1,1} C_1^{l+1}(x) + I^{l+1} \right)^\top \dots \quad (53)$$

$$\left(\alpha^{\frac{m}{2}} \sqrt{\frac{2^{m-1}}{\prod_{h'=0}^{m-1} n_{l,h'}}} W^{l+1,1} C_1^{l+1}(x') + I^{l+1} \right) A^{l+2}(x') \quad (54)$$

$$= \alpha^{\frac{m}{2}} \sqrt{\frac{2^{m-1}}{\prod_{h'=0}^{m-1} n_{l,h'}}} A^{l+2}(x)^\top C_1^{l+1}(x)^\top W^{l+1,1\top} I^{l+1} A^{l+2}(x') \quad (55)$$

$$+ \alpha^{\frac{m}{2}} \sqrt{\frac{2^{m-1}}{\prod_{h'=0}^{m-1} n_{l,h'}}} A^{l+2}(x')^\top C_1^{l+1}(x')^\top W^{l+1,1\top} I^{l+1} A^{l+2}(x) \quad (56)$$

$$+ \alpha^m \frac{2^{m-1}}{\prod_{h'=0}^{m-1} n_{l,h'}} A^{l+2}(x)^\top C_1^{l+1}(x)^\top W^{l+1,1\top} W^{l+1,1} C_1^{l+1}(x') A^{l+2}(x') \quad (57)$$

$$+ \langle A^{l+2}(x), A^{l+2}(x') \rangle \quad (58)$$

$$= T_1 + T_2 + T_3 + T_4 \quad (59)$$

Note that $\sqrt{\frac{1}{n_l}} \|W^{l+1,1\top} I^{l+1\top}\| \rightarrow 0$ as n_l tends to infinity, and so $T_1, T_2 \rightarrow 0$. Taking $n_{l+1} \rightarrow \infty$, we have $\frac{1}{n_l} W^{l+1,1\top} W^{l+1,1} \rightarrow I$. Taking $n_0 \dots n_{l,m} \rightarrow \infty$, we have that $T_3 \rightarrow \prod_{h'=1}^{m-1} \dot{\Sigma}^{l,h'}(x, x') \langle A^{l+2}(x), A^{l+2}(x') \rangle$.

And so it follows:

$$\lim_{n_0 \dots n_L \rightarrow \infty} \langle A^{l+1}(x), A^{l+1}(x') \rangle = \lim_{n_0 \dots n_L \rightarrow \infty} \langle A^{l+2}(x), A^{l+2}(x') \rangle \left(\alpha^m \prod_{h'=1}^{m-1} \dot{\Sigma}^{l,h'}(x, x') + I \right) \quad (60)$$

$$= \prod_{l'=l}^{L-1} \left(\alpha^m \prod_{h'=1}^{m-1} \dot{\Sigma}^{l',h'}(x, x') + I \right) \lim_{n_L \rightarrow \infty} \frac{1}{n_L} W^{f\top} W^f = \prod_{l'=l}^{L-1} \left(\alpha^m \prod_{h'=1}^{m-1} \dot{\Sigma}^{l',h'}(x, x') + I \right) \quad (61)$$

And finally:

$$\begin{aligned} \lim_{n_0 \dots n_L \rightarrow \infty} \left\langle \frac{\partial f(x, W)}{\partial W^{l,h}}, \frac{\partial f(x', W)}{\partial W^{l,h}} \right\rangle \\ = \alpha^m \Sigma^{l-1,h-1}(x, x') \prod_{h'=h}^{m-1} \dot{\Sigma}^{l-1,h'}(x, x') \prod_{l'=l}^{L-1} \left(\alpha^m \prod_{h'=1}^{m-1} \dot{\Sigma}^{l',h'}(x, x') + I \right) \end{aligned} \quad (62)$$

The derivation for the case of $h = 1$ gives an identical result, and so summing over all the weights:

$$\begin{aligned} K_L^R(x, x') &= \lim_{n_0 \dots n_L \rightarrow \infty} \sum_{l=1}^L \sum_{h=1}^m \left\langle \frac{\partial f(x, W)}{\partial W^{l,h}}, \frac{\partial f(x', W)}{\partial W^{l,h}} \right\rangle \\ &= \alpha^m \sum_{l=1}^L \sum_{h=1}^m \left(\Sigma^{l-1,h-1}(x, x') \prod_{h'=h}^{m-1} \dot{\Sigma}^{l-1,h'}(x, x') \right) \prod_{l'=l}^{L-1} \left(\alpha^m \prod_{h'=1}^{m-1} \dot{\Sigma}^{l',h'}(x, x') + 1 \right) \\ &= K_{L-1}^R(x, x') \left(\alpha^m \prod_{h=1}^{m-1} \dot{\Sigma}^{L-1,h}(x, x') + 1 \right) + \alpha^m \sum_{h=1}^m \left(\Sigma^{L,h-1}(x, x') \prod_{h'=h}^{m-1} \dot{\Sigma}^{L,h'}(x, x') \right) \end{aligned} \quad (63)$$

For the diagonal elements $K(x, x)$, note that:

$$\Sigma^{l,h+1}(x, x) = 2 \mathbb{E}_{u,v \sim \mathcal{N}(0, \Sigma^{l,h})} [\phi(u)\phi(u)] = \Sigma^{l,h}(x, x) = \Sigma^l(x, x) \quad (64)$$

and:

$$\dot{\Sigma}^{l,h+1}(x, x) = 2 \mathbb{E}_{u \sim \mathcal{N}(0, \Sigma^{l,h})} [\dot{\phi}(u)\dot{\phi}(u)] = 1 \quad (65)$$

Recalling the relation:

$$\begin{aligned}\Sigma^l(x, x') &= \Sigma^{l-1}(x, x') + \alpha^m \Sigma^{l-1,m}(x, x') \\ &\rightarrow \Sigma^l(x, x) = \Sigma^{l-1}(x, x) + \alpha^m \Sigma^{l-1,m}(x, x) = \Sigma^{l-1}(x, x) (1 + \alpha^m)\end{aligned}\quad (66)$$

yielding:

$$K(x, x') = Lm\alpha^m (1 + \alpha^m)^{L-1} \quad (67)$$

□

A.2. Proof of Theorem 2

Proof. Similarly to the ResNet case, the derivative $\frac{\partial f(x, W)}{\partial W^{l,h}}$ can be written in a compact matrix form:

$$\forall_{0 \leq h < l \leq L}, \frac{\partial f(x, W)}{\partial W^{l,h}} = \sqrt{\frac{1}{ln'_{l-1}}} [q^h(x)]_{n'_{l-1}} (A^{l+1,l}(x))^\top \quad (68)$$

where:

$$A^{l,h}(x) = \begin{cases} \sqrt{\frac{2}{ln'_{l-1}}} Z^h(x) I^{h,l-1} W^{l,h} A^{l+1,l}(x) + A^{l+1,h}(x) & 0 \leq h < l < L \\ \sqrt{\frac{2}{ln'_{l-1}}} Z^h(x) I^{h,l-1} W^{l,h} A^{l+1,l}(x) & l = L \\ \frac{1}{\sqrt{n_L}} W^f & l = L + 1 \end{cases} \quad (69)$$

where Z^l is a diagonal matrix holding the binary activation variables of layer l in its diagonal, and $I^{h,l} = [I_{n'_l}; \mathbf{0}_{n_h - n'_l}]^\top \in \mathbb{R}^{n_h \times n'_l}$ is a concatenation of an n_h dimensional identity matrix, and a zero matrix $\mathbf{0}_{n_h - n'_l} \in \mathbb{R}^{n'_l \times n_h - n'_l}$. We then have:

$$\forall_{0 \leq h < l \leq L}, \left\langle \frac{\partial f(x, W)}{\partial W^{l,h}}, \frac{\partial f(x', W)}{\partial W^{l,h}} \right\rangle = \frac{1}{ln'_{l-1}} \left\langle [q^h(x)]_{n'_{l-1}}, [q^h(x')]_{n'_{l-1}} \right\rangle \left\langle A^{l+1,l}(x), A^{l+1,l}(x') \right\rangle \quad (70)$$

after taking the limit $n_0, n'_1, \dots, n'_{L-1} \rightarrow \infty$, it holds that $\frac{1}{ln'_{l-1}} \left\langle [q^h(x)]_{n'_{l-1}}, [q^h(x')]_{n'_{l-1}} \right\rangle \rightarrow \frac{1}{l} \Sigma^h(x, x')$. We are left with computing the limit of $\left\langle A^{l+1,l}(x), A^{l+1,l}(x') \right\rangle$. It follows that:

$$\begin{aligned}\forall_{0 \leq h < l < L}, \left\langle A^{l,h}(x), A^{l,h}(x') \right\rangle &= \sqrt{\frac{2}{ln'_{l-1}}} A^{l+1,h\top}(x) Z^h(x') I^{h,l-1} W^{l,h} A^{l+1,l}(x') \\ &+ \left\langle A^{l,h}(x), A^{l,h}(x') \right\rangle = \sqrt{\frac{2}{ln'_{l-1}}} A^{l+1,h\top}(x') Z^h(x) I^{h,l-1} W^{l,h} A^{l+1,l}(x) \\ &+ \frac{2}{ln'_{l-1}} A^{l+1,l\top}(x) W^{l,h\top} I^{h,l-1\top} Z^h(x) Z^h(x') I^{h,l-1} W^{l,h} A^{l+1,l}(x') + A^{l+1,h\top}(x) A^{l+1,h}(x') \\ &= T_1 + T_2 + T_3 + T_4\end{aligned}\quad (71)$$

Expanding T_1 :

$$\begin{aligned}
 T_1 &= \sqrt{\frac{2}{ln'_{l-1}}} A^{l+1,h\top}(x) Z^h(x') I^{h,l-1} W^{l,h} A^{l+1,l}(x') \\
 &= \left(\sqrt{\frac{2}{(l+1)n'_l}} Z^h(x) I^{h,l} W^{l+1,h} A^{l+2,l+1}(x) + A^{l+2,h}(x) \right)^\top \sqrt{\frac{2}{ln'_{l-1}}} Z^h(x') I^{h,l-1} W^{l,h} A^{l+1,l}(x') \\
 &= \frac{2}{\sqrt{l(l+1)n'_{l-1}n'_l}} A^{l+2,l+1\top}(x) W^{l+1,h\top} I^{h,l\top} Z^h(x) Z^h(x') I^{h,l-1} W^{l,h} A^{l+1,l}(x') \\
 &\quad + A^{l+2,h}(x)^\top \sqrt{\frac{2}{ln'_{l-1}}} Z^h(x') I^{h,l-1} W^{l,h} A^{l+1,l}(x') \quad (72)
 \end{aligned}$$

Looking at the first term of the expansion, notice that after taking the limit $n_0 \dots n'_{l-1} \rightarrow \infty$, it holds that $\frac{1}{\sqrt{n'_{l-1}}} \|I^{h,l\top} Z^h(x) Z^h(x') I^{h,l-1} W^{l,h}\| \rightarrow 0$, and so we are left with the second term:

$$\lim_{n_0 \dots n'_{l-1} \rightarrow \infty} T_1 = \lim_{n_0 \dots n'_{l-1} \rightarrow \infty} A^{l+2,h}(x)^\top \sqrt{\frac{2}{ln'_{l-1}}} Z^h(x') I^{h,l-1} W^{l,h} A^{l+1,l}(x') \quad (73)$$

Recursively expanding $A^{l+2,h}(x)$, we get similar terms that vanish in the limit, therefore:

$$\lim_{n_0 \dots n'_{l-1} \rightarrow \infty} T_1 = \lim_{n_0 \dots n'_{l-1} \rightarrow \infty} A^{L,h}(x)^\top \sqrt{\frac{2}{ln'_{l-1}}} Z^h(x') I^{h,l-1} W^{l,h} A^{l+1,l}(x') \rightarrow 0 \quad (74)$$

And so $\lim_{n_0 \dots n'_{l-1} \rightarrow \infty} T_1, T_2 \rightarrow 0$. We are left with evaluating the limit of T_3, T_4 . Expanding T_3 :

$$\lim_{n_0 \dots n'_{l-1} \rightarrow \infty} T_3 = \lim_{n_0 \dots n'_{l-1} \rightarrow \infty} \frac{2}{ln'_{l-1}} A^{l+1,l\top}(x) W^{l,h\top} I^{h,l-1\top} Z^h(x) Z^h(x') I^{h,l-1} W^{l,h} A^{l+1,l}(x') \quad (75)$$

Note that it holds that $\lim_{n_0 \dots n'_{l-1} \rightarrow \infty} \frac{2}{n'_{l-1}} W^{l,h\top} I^{h,l-1\top} Z^h(x) Z^h(x') I^{h,l-1} W^{l,h} \rightarrow \dot{\Sigma}^h(x, x') I$, and so:

$$\lim_{n_0 \dots n'_{l-1} \rightarrow \infty} T_3 = \frac{\dot{\Sigma}^h(x, x')}{l} A^{l+1,l\top}(x) A^{l+1,l}(x') \quad (76)$$

Plugging back into Eq. 71:

$$\lim_{n_0 \dots n'_{l-1} \rightarrow \infty} \langle A^{l,h}(x), A^{l,h}(x') \rangle = \lim_{n_0 \dots n'_{l-1} \rightarrow \infty} T_3 + T_4 \quad (77)$$

$$= \frac{\dot{\Sigma}^h(x, x')}{l} \langle A^{l+1,l}(x), A^{l+1,l}(x') \rangle + \langle A^{l+1,h}(x), A^{l+1,h}(x') \rangle \quad (78)$$

and:

$$\lim_{n_0 \dots n_L \rightarrow \infty} \langle A^{L,h}(x), A^{L,h}(x') \rangle = \lim_{n_0 \dots n_L \rightarrow \infty} T_3 \quad (79)$$

$$= \lim_{n_0 \dots n_L \rightarrow \infty} \frac{\dot{\Sigma}^h(x, x')}{L} \langle A^{L+1,l}(x), A^{L+1,l}(x') \rangle = \frac{\dot{\Sigma}^h(x, x')}{L} \quad (80)$$

Denoting by $m^{l,h}(x, x') = \lim_{n_0 \dots n_L \rightarrow \infty} \langle A^{l,h}(x), A^{l,h}(x') \rangle$, it holds that:

$$\lim_{n_0 \dots n_L \rightarrow \infty} m_{L+1,h} = \frac{1}{n_L} W^{f\top} W^f = 1 \quad (81)$$

Plugging into Eq. 70, we arrive at:

$$\lim_{n_0 \dots n_L \rightarrow \infty} \left\langle \frac{\partial f(x, W)}{\partial W^{l,h}}, \frac{\partial f(x', W)}{\partial W^{l,h}} \right\rangle = \frac{1}{l} \Sigma^h(x, x') m^{l+1,l}(x, x') \quad (82)$$

with the following recursion:

$$m_{l,h}(x, x') = \begin{cases} \frac{\dot{\Sigma}^h(x, x')}{l} m^{l+1,l}(x, x') + m^{l+1,h}(x, x') & 0 \leq h < l < L \\ \frac{\dot{\Sigma}^h(x, x')}{L} & 0 \leq h < L, l = L \end{cases} \quad (83)$$

Summing over all the weights, we have:

$$K_L^D(x, x') = \sum_{l=1}^L \frac{\sum_{h=0}^{l-1} \Sigma^h(x, x')}{l} m^{l+1,l}(x, x') \quad (84)$$

Note that:

$$\dot{\Sigma}^l(x, x) = 2 \mathbb{E}_{u, v \sim \mathcal{N}(0, \frac{\Sigma^l(x, x')}{l-1})} [\phi(u) \phi(u)] = 1 \quad (85)$$

and:

$$\Sigma^1(x, x) = 2 \mathbb{E}_{u, v \sim \mathcal{N}(0, \Sigma^0(x, x))} [\phi(u) \phi(u)] = x^\top x = 1 \quad (86)$$

$$\Sigma^{l+1}(x, x) = 2 \mathbb{E}_{u, v \sim \mathcal{N}(0, \frac{\Sigma^l(x, x)}{l})} [\phi(u) \phi(u)] = 1 \quad (87)$$

Plugging into Eq. 83:

$$\forall_{0 \leq h \leq L-1} m^{L-1,h}(x, x) = \frac{1}{(L-1)L} + \frac{1}{L} = \frac{1}{L-1} \quad (88)$$

(89)

$$\forall_{0 \leq h \leq L-2} m^{L-2,h}(x, x) = \frac{1}{L-2} \frac{1}{L-1} + \frac{1}{L-1} = \frac{1}{L-2} \quad (90)$$

Recurse through $l = L \dots l+1$:

$$\forall_{0 \leq l \leq L} m^{l+1,l}(x, x) = \frac{1}{l+1} \quad (91)$$

Plugging into Eq. 70:

$$\forall_{0 \leq h < l \leq L}, \lim_{n_0 \dots n_L \rightarrow \infty} \left\langle \frac{\partial f(x, W)}{\partial W^{l,h}}, \frac{\partial f(x, W)}{\partial W^{l,h}} \right\rangle = \frac{1}{l(l+1)} \quad (92)$$

finally:

$$K_L^D(x, x) = \sum_{l=1}^L \frac{1}{l+1} \quad (93)$$

□

A.3. Proof of lemma 1

Proof. Smoothness of f implies that for any u, v it holds $\|\nabla f(u) - \nabla f(v)\| \leq \frac{\beta}{2} \|u - v\|$, and the following hold:

$$f(v) \leq f(u) + \langle \nabla f(u), v - u \rangle + \frac{\beta}{2} \|v - u\|^2 \quad (94)$$

Setting $v = u - \frac{1}{\beta} \nabla f(u)$, we have (using the fact that $f \geq 0$):

$$\|\nabla f(u)\| \leq \sqrt{2\beta f(u)} \quad (95)$$

together with the assumption that $\|\nabla f(u)\| \geq \sqrt{2c\beta f(u)}$, we have:

$$\sqrt{2c\beta f(u)} \leq \|\nabla f(u)\| \leq \sqrt{2\beta f(u)} \quad (96)$$

Setting $v = u - \alpha \nabla f(u)$ in Eq. 94:

$$f(v) \leq f(u) - \alpha \|\nabla f(u)\|^2 \left(1 - \frac{\alpha\beta}{2}\right) \leq f(u) - 2c\alpha\beta f(u) \left(1 - \frac{\alpha\beta}{2}\right) \quad (97)$$

$$= f(u) \left(1 - 2c\alpha\beta \left(1 - \frac{\alpha\beta}{2}\right)\right) \quad (98)$$

For $0 \leq \alpha < \frac{1}{\beta}$, it holds that $0 \leq \left(1 - 2c\alpha\beta \left(1 - \frac{\alpha\beta}{2}\right)\right) < 1$, and so It follows:

$$f(u_\infty) \leq f(u_0) \left(1 - 2c\alpha\beta \left(1 - \frac{\alpha\beta}{2}\right)\right)^\infty = 0 \quad (99)$$

□

For the sake of clarity, we present the proofs of Theorems 3 and 4 for a depth L ResNet with $m = 2$. The extension for other residual architectures discussed in the paper is straightforward and requires no additional arguments.

We make use of the following propositions and definitions to aid in the proofs.

proposition 1. *Given a random vector $w = [w_1 \dots w_n]$ such that each component is identically and symmetrically distributed i.i.d random variable with moments $\mathbb{E}(w_i^m) = c_m$ ($c_0 = 1, c_1 = 0, c_2 = 1$), a set of non negative integers $m_1 \dots m_l$ such that $\sum_{i=1}^l m_i$ is even, and a random binary variable $z \in \{0, 1\}$ such that $(z|w) = 1 - (z| - w)$, then it holds that:*

$$\mathbb{E}\left[\prod_{i=1}^l w_i^{m_i} z\right] = \frac{\prod_{i=1}^l c_{m_i}}{2} \quad (100)$$

Proof. We have:

$$\prod_{i=1}^l c_{m_i} = \int_w \prod_{i=1}^l w_i^{m_i} p(w) dw = \int_{w|z=1} \prod_{i=1}^l w_i^{m_i} p(w) dw + \int_{w|z=0} \prod_{i=1}^l w_i^{m_i} p(w) dw \quad (101)$$

$$= \int_{w|z=1} \prod_{i=1}^l w_i^{m_i} p(w) dw + \int_{w|z=1} \prod_{i=1}^l (-w_i)^{m_i} p(w) dw \quad (102)$$

$$= \int_w \prod_{i=1}^l w_i^{m_i} z p(w) dw + \int_w \prod_{i=1}^l (-w_i)^{m_i} z p(w) dw \quad (103)$$

For even $\sum_{i=1}^l m_i$, it follows that:

$$\int_w \prod_{i=1}^l (-w_i)^{m_i} z p(w) dw = \int_w \prod_{i=1}^l w_i^{m_i} z p(w) dw \quad (104)$$

and so:

$$\prod_{i=1}^l c_{m_i} = 2 \int_w \prod_{i=1}^l w_i^{m_i} z p(w) dw \quad (105)$$

giving rise to:

$$\frac{\prod_{i=1}^l c_{m_i}}{2} = \int_w \prod_{i=1}^l w_i^{m_i} z p(w) dw = \mathbb{E}\left[\prod_{i=1}^l w_i^{m_i} z\right] \quad (106)$$

□

proposition 2. *Given a random vector $w = [w_1 \dots w_n]$ such that each component is identically and symmetrically distributed i.i.d random variable with moments $\mathbb{E}(w_i^m) = c_m$ ($c_0 = 1, c_1 = 0, c_2 = 1$), two sets of non negative integers $m_1 \dots m_l, n_1 \dots n_l$, such that $\sum_{i=1}^l m_i, \sum_{i=1}^l n_i$ are even, $\forall i, m_i \geq n_i$, and a random binary variable $z \in \{0, 1\}$, such that $(z|w) = 1 - (z| - w)$, then it holds that:*

$$\mathbb{E}\left[\frac{1}{w_i^{n_i}} \prod_{i=1}^l w_i^{m_i} z\right] = \frac{\prod_{i=1}^l c_{m_i - n_i}}{2} \quad (107)$$

Proof. This is trivially true from proposition 1 since $\sum_i (m_i - n_i)$ is even. □

Definition 2. *A path γ from input to output defines a product of weights along the path denoted by*

$$P_\gamma = \prod_{l=1}^{|\gamma|} \hat{p}_{\gamma,l} = z_\gamma \prod_{l=1}^{|\gamma|} (w_{\gamma,l}^1 w_{\gamma,l}^2) \quad (108)$$

where $|\gamma|$ is the length of path γ (for vanilla and DenseNets $|\gamma| = L$), z_γ is a binary variable $z_\gamma \in \{0, 1\}$ indicating if the path is “active” (i.e., all relevant ReLU activations along the path are open), and $w_{\gamma, l}^1, w_{\gamma, l}^2$ are the weights along path γ associated with some residual branch.

We generalize the above expression the following way:

$$P_\gamma = \prod_{l=0}^L p_{\gamma, l} \quad (109)$$

where:

$$p_{\gamma, l} = \begin{cases} 1 & l \notin \gamma \\ w_{\gamma, 0}^1 w_{\gamma, 0}^2 & l = 0 \\ w_{\gamma, l}^1 z_{\gamma, l} w_{\gamma, l}^2 & \text{else} \end{cases} \quad (110)$$

Here, $w_{\gamma, l}^1, w_{\gamma, l}^2$ are weights associated with residual branch l , $W^{l,1}, W^{l,2}$ ($w_{\gamma, 0}^1, w_{\gamma, 0}^2$ belong to the first and last linear projection matrices W^s, W^f), and $z_{\gamma, l}$ is the binary activation variable relevant for weight $w_{\gamma, l}^1$. (Note that $z_{\gamma, l}$ depends on $w_{\gamma, l}^1$ but not on $w_{\gamma, l}^2$). $l \notin \gamma$ indicates if layer l is skipped. Since both $f_{(k)}$ and f^k are comprised from a sum over the same paths from input to output (with different activation patterns), the m 'th moment of both is an expectation over sum of m -product of paths.

proposition 3. For any set of m paths $\gamma^1 \dots \gamma^m$, there exists an integer $0 \leq s \leq m$, a series of non negative integers $\{m_{u,v}\}$ and $\{m_v\}$ where $\sum_u m_{u,v} = m_v$, $\sum_v m_v = s$, i.i.d random variables $\{w_u\}, \{w_v\}$ with moments $\forall_{u,v}, \mathbb{E}[w_u^t] = \mathbb{E}[w_v^t] = c_t$ and a binary random variable $z \in \{0, 1\}$ where $(z|\{w_u\}) = 1 - (z|\{-w_u\})$, such that:

$$\forall_{1 \leq l \leq L} \mathbb{E}_{\mathcal{N}} \left[\prod_{i=1}^m p_{\gamma^i, l} \middle| \|y^{l-1}\| > 0 \right] = \prod_v \left(\mathbb{E}_{\mathcal{N}} \left[\prod_{u=1}^s w_u^{m_{u,v}} z \right] \mathbb{E}_{\mathcal{N}} [w_v^{m_v}] \right) = \frac{\prod_v c_{m_v} \prod_{u,v} c_{m_{u,v}}}{2} \quad (111)$$

where $\mathbb{E}_{\mathcal{N}}$ stands for expectation using the full architecture. Moreover, it holds for $1 \leq k \leq L$:

$$\forall_{l \neq k} \mathbb{E}_{\mathcal{N}_{(k)}} \left[\prod_{i=1}^m p_{\gamma^i, l} \middle| \|y_{(k)}^{l-1}\| > 0 \right] = \prod_v \left(\mathbb{E}_{\mathcal{N}_{(k)}} \left[\prod_{u=1}^s w_u^{m_{u,v}} z \right] \mathbb{E}[w_v^{m_v}] \right) = \frac{\prod_v c_{m_v} \prod_{u,v} c_{m_{u,v}}}{2} \quad (112)$$

where $\mathbb{E}_{\mathcal{N}_{(k)}}$ stands for expectation using the reduced architecture.

Proof. Rearranging the set of paths, such that $\forall_{1 \leq i \leq s}, p_{\gamma_i, l} \neq 1$ and $\forall_{s < i \leq m}, p_{\gamma_i, l} = 1$ where $s \leq m$, it holds:

$$\mathbb{E}_{\mathcal{N}} \left[\prod_{i=1}^m p_{\gamma^i, l} \middle| \|y^{l-1}\| > 0 \right] = \mathbb{E}_{\mathcal{N}} \left[\prod_{i=1}^s p_{\gamma^i, l} \middle| \|y^{l-1}\| > 0 \right] \quad (113)$$

$$= \mathbb{E}_{\mathcal{N}} \left[\prod_{i=1}^s (w_{\gamma^i, l}^1 z_{\gamma^i, l} w_{\gamma^i, l}^2) \middle| \|y^{l-1}\| > 0 \right] = \mathbb{E}_{\mathcal{N}} \left[\prod_{i=1}^s (w_{\gamma^i, l}^1 z_{\gamma^i, l}) \middle| \|y^{l-1}\| > 0 \right] \mathbb{E}_{\mathcal{N}} \left[\prod_{i=1}^s w_{\gamma^i, l}^2 \right] \quad (114)$$

Let $\{w_v\}$ be the set of unique weights out of the set $\{w_{\gamma^i, l}^2\}$, with corresponding multiplicity $\{m_v\}$. Note that there is a 1 to 1 correspondence between the set $\{w_v\}$, and the set of unique activation $\{z_v\}$. For every z_v , we denote the set of unique variables $\{w_{u,v}\}$ out of the set $\{w_{\gamma^i, l}^1\}$ associated with z_v , with corresponding multiplicity $\{m_{u,v}\}$. Since when conditioned on y^{l-1} , the set of activation variables $\{z_v\}$ are independent. It then follows:

$$\mathbb{E}_{\mathcal{N}} \left[\prod_{i=1}^m p_{\gamma^i, l} \middle| \|y^{l-1}\| > 0 \right] = \prod_v \left(\mathbb{E}_{\mathcal{N}} \left[\prod_{u=1}^s w_u^{m_{u,v}} z_v \right] \mathbb{E}_{\mathcal{N}} [w_v^{m_v}] \right) = \prod_v \mathbb{E}_{\mathcal{N}} \left[\prod_{u=1}^s w_u^{m_{u,v}} z_v \right] \prod_v c_{m_v} \quad (115)$$

note that for both the full and reduced architectures, flipping the sign of $W^{l,1} y^{l-1}$ will flip the activation variables (except for a set of zero measure defined by $W^{l,1\top} y^{l-1} = 0$ which does not affect the expectation). From the symmetry of the distribution of the weights, if c_{m_v} is non zero, then by definition $m_v = \sum_u m_{u,v}$ is even. We can then apply proposition 1:

$$\mathbb{E}_{\mathcal{N}} \left[\prod_{i=1}^m p_{\gamma^i, l} \middle| \|y^{l-1}\| > 0 \right] = \prod_v \mathbb{E}_{\mathcal{N}} \left[\prod_{u=1}^s w_u^{m_{u,v}} z_v \right] \prod_v c_{m_v} = \frac{\prod_v c_{m_v} \prod_{u,v} c_{m_{u,v}}}{2}. \quad (116)$$

The proof for the reduced architecture follows the same derivation, and is, therefor, also correct. \square

A.4. Proof of Theorem 3

we aim to show that for an even m :

$$\mathbb{E} [\|f_{(k)}\|^m] = \mathbb{E} [\|f^k\|^m] \quad (117)$$

where $f_{(k)}$ is the output of the reduced network, and f^k is the contributions of paths going through weight W^k , out of the full output f . We similarly define the intermediate outputs in both cases $\{y^{k,l}\}_{l=0}^L$, and $\{y_{(k)}^l\}_{l=0}^L$.

We denote a set of m paths from input to output by $\gamma^1 \dots \gamma^m$, where m is even. Since the computations done by all considered architectures form a markov chain, such that the output of any layer depends only on up-stream weights, denoted by R^l . We aim to show that:

$$\mathbb{E}_{\mathcal{N}_{(k)}} [\prod_{i=1}^m P_{\gamma^i}] = \mathbb{E}_{\mathcal{N}} [\prod_{i=1}^m P_{\gamma^i}] \quad (118)$$

That is, the expectation of the product is the same both the reduced architecture, and the original.

Using conditional expectation:

$$\mathbb{E}_{\mathcal{N}} [\prod_{i=1}^m P_{\gamma^i}] = \mathbb{E}_{\mathcal{N}} [\prod_{l=0}^L \prod_{i=1}^m p_{\gamma^i, l}] = \mathbb{E}_{\mathcal{N}} [\prod_{l=0}^{L-1} \prod_{i=1}^m p_{\gamma^i, l} \mathbb{E}_{\mathcal{N}} [\prod_{i=1}^m p_{\gamma^i, L} \mid R^{L-1}]] \quad (119)$$

Using proposition 3, we have:

$$\mathbb{E}_{\mathcal{N}} [\prod_{i=1}^m p_{\gamma^i, L} \mid R^{L-1}] = \mathbb{1}_{\|y^{L-1}\| > 0} \frac{\prod_v c_{m_v} \prod_{u,v} c_{m_{u,v}}}{2} \quad (120)$$

and so:

$$\mathbb{E}_{\mathcal{N}} [\prod_{i=1}^m P_{\gamma^i}] = \frac{\prod_v c_{m_v} \prod_{u,v} c_{m_{u,v}}}{2} \mathbb{E}_{\mathcal{N}} [\mathbb{1}_{\|y^{L-1}\| > 0} \prod_{l=0}^{L-1} \prod_{i=1}^m p_{\gamma^i, l}] \quad (121)$$

$$= \frac{\prod_v c_{m_v} \prod_{u,v} c_{m_{u,v}}}{2} \mathbb{E}_{\mathcal{N}} [\prod_{l=0}^{L-1} \prod_{i=1}^m p_{\gamma^i, l}] = \mathbb{E}_{\mathcal{N}_{(k)}} [\prod_{i=1}^m P_{\gamma^i}] \quad (122)$$

Recurse through $L-1 \dots 1$ completes the proof.

A.5. proof of Theorem 4

Proof. Neglecting scaling coefficients for simplicity, the expectation of the squared output $f_{(k)}$ can be expressed using proposition 3:

$$\mathbb{E}[(f^k)^2] = \mathbb{E} \left[\left(\sum_{i,j} \sum_{w_{i,j}^{k,1} \in \gamma} P_{\gamma} \right)^2 \right] = \sum_{i,j} \sum_{w_{i,j}^{k,1} \in \gamma} \mathbb{E}[P_{\gamma}^2] = \frac{1}{2^L} \sum_{i,j} \sum_{w_{i,j}^{k,1} \in \gamma} = \mathbb{E}[(f_{(k)})^2] \quad (123)$$

The Jacobian $J^{k,1}$ can be expressed using proposition 3:

$$\mathbb{E} \left[\left\| \frac{\partial f^k}{\partial W^{k,1}} \right\|^2 \right] = \sum_{i,j} \mathbb{E} \left[\left(\sum_{w_{i,j}^{k,1} \in \gamma} \frac{1}{w_{i,j}^{k,1}} P_{\gamma} \right)^2 \right] \quad (124)$$

$$= \sum_{i,j} \sum_{w_{i,j}^{k,1} \in \gamma} \mathbb{E} \left[\left(\frac{1}{w_{i,j}^{k,1}} p_{\gamma,k} \right)^2 \mid \|y^{k-1}\| > 0 \right] \prod_{l \neq k}^L \mathbb{E} \left[(p_{\gamma,l})^2 \mid \|y^{l-1}\| > 0 \right] \quad (125)$$

$$= \sum_{i,j} \sum_{w_{i,j}^{k,1} \in \gamma} \mathbb{E} \left[\frac{1}{(w_{i,j}^{k,1})^2} (w_{i,j}^{k,1})^2 (z_{\gamma} \mid \|y^{k-1}\| > 0) \right] \frac{1}{2^{L-1}} \quad (126)$$

Using Proposition 2:

$$\mathbb{E} \left[\left\| \frac{\partial f^k}{\partial W^{k,1}} \right\|^2 \right] = \frac{1}{2^{L-1}} \sum_{i,j} \sum_{w_{i,j}^{k,1} \in \gamma} \frac{c_0}{2} = \frac{1}{2^L} \sum_{i,j} \sum_{w_{i,j}^{k,1} \in \gamma} = \mathbb{E}[(f_{(k)})^2] \quad (127)$$

Expanding the fourth moment:

$$\mathbb{E} \left[\left\| \frac{\partial f^k}{\partial W^{k,1}} \right\|^4 \right] = \sum_{i,j} \sum_{u,v} \mathbb{E} \left[\left(\sum_{w_{i,j}^{k,1} \in \gamma} \frac{1}{w_{i,j}^{k,1}} P_\gamma \right)^2 \left(\sum_{w_{u,v}^{k,1} \in \gamma} \frac{1}{w_{u,v}^{k,1}} P_\gamma \right)^2 \right] \quad (128)$$

$$= \sum_{i,j} \sum_{u,v} \mathbb{E} \left[\frac{1}{(w_{i,j}^{k,1})^2 (w_{u,v}^{k,1})^2} \sum_{w_{i,j}^{k,1} \in \gamma^1, \gamma^2} \sum_{w_{u,v}^{k,1} \in \gamma^3, \gamma^4} P_{\gamma^1} P_{\gamma^2} P_{\gamma^3} P_{\gamma^4} \right] \quad (129)$$

Finally, using Proposition 3:

$$\mathbb{E} \left[\left\| \frac{\partial f^k}{\partial W^{k,1}} \right\|^4 \right] \geq \frac{1}{c_4} \sum_{i,j} \sum_{u,v} \mathbb{E} \left[\sum_{w_{i,j}^{k,1} \in \gamma^1, \gamma^2} \sum_{w_{u,v}^{k,1} \in \gamma^3, \gamma^4} P_{\gamma^1} P_{\gamma^2} P_{\gamma^3} P_{\gamma^4} \right] = \frac{1}{c_4} \mathbb{E} \left[\|f_{(k)}\|^4 \right] \quad (130)$$

□

We use the following proposition to aid in the proofs of Theorems 5 and 6.

proposition 4. *For vanilla fully connected network, with intermediate outputs given by:*

$$\forall_{0 \leq l \leq L}, y^l = \sqrt{2} \phi \left(\frac{1}{\sqrt{n_{l-1}}} W^{l\top} y^{l-1} \right) \quad (131)$$

, where the weight matrices $W^l \in \mathbb{R}^{n_{l-1} \times n_l}$ are normally distributed, the following holds at initialization:

$$\mathbb{E}[\|y^l\|^2] = \frac{n_l}{n_{l-1}} \mathbb{E}[\|y^{l-1}\|^2] \quad (132)$$

$$\mathbb{E}[\|y^l\|^4] = \frac{n_l(n_l + 5)}{n_{l-1}^2} \mathbb{E}[\|y^{l-1}\|^4] \quad (133)$$

Proof. Absorbing the scale $\sqrt{\frac{2}{n_{l-1}}}$ into the weights, we denote by Z^l the diagonal matrix holding in its diagonal the activation variables z_j^l for unit j in layer l , and so we have:

$$y^l = Z^l W^{l\top} y^{l-1} \quad (134)$$

Conditioning on $R^{l-1} = \{W^1 \dots W^{l-1}\}$ and taking expectation:

$$\mathbb{E}[\|y^l\|^2 | R^{l-1}] = y^{l-1\top} \mathbb{E} \left[W^l Z^l W^{l\top} \right] y^{l-1} \quad (135)$$

$$= \sum_{j=1}^{n_l} \sum_{i_1, i_2=1}^{n_{l-1}} y_{i_1}^{l-1} y_{i_2}^{l-1} \mathbb{E} \left[w_{i_1, j}^l w_{i_2, j}^l z_j^l | R^{l-1} \right] \quad (136)$$

From Proposition 1, it follows that:

$$\mathbb{E}[\|y^l\|^2] = \mathbb{E} \left[\mathbb{E}[\|y^l\|^2 | R^{l-1}] \right] = \frac{n_L}{n_{L-1}} \mathbb{E}[\|y^{l-1}\|^2] \quad (137)$$

Similarly:

$$\mathbb{E} \left[\|y^l\|^4 | R^{l-1} \right] = \mathbb{E} \left[(y^{L-1\top} W^L Z^L W^{L\top} y^{L-1})^2 | R^{l-1} \right] \quad (138)$$

$$= \sum_{j_1, j_2, i_1, i_2, i_3, i_4} y_{i_1}^{l-1} y_{i_2}^{l-1} y_{i_3}^{L-1} y_{i_4}^{L-1} \mathbb{E} \left[w_{i_1, j_1}^l w_{i_2, j_1}^l w_{i_3, j_2}^l w_{i_4, j_2}^l z_{j_1}^l z_{j_2}^l | R^{l-1} \right] \quad (139)$$

From Proposition 1, and the independence of the activation variables conditioned on R^{l-1} :

$$\mathbb{E} \left[w_{i_1, j_1}^l w_{i_2, j_1}^l w_{i_3, j_2}^l w_{i_4, j_2}^l z_{j_1}^l z_{j_2}^l | R^{l-1} \right] \quad (140)$$

$$= \mathbb{E} \left[w_{i_1, j_1}^l w_{i_2, j_1}^l w_{i_3, j_2}^l w_{i_4, j_2}^l z_{j_1}^l z_{j_2}^l | R^{l-1} \right] \left(\mathbb{1}_{j_1=j_2, i_1=i_2=i_3=i_4} + 3 \mathbb{1}_{j_1=j_2, i_1=i_2, i_3=i_4, i_1 \neq i_3} \dots \right. \quad (141)$$

$$\left. + \mathbb{1}_{j_1 \neq j_2, i_1=i_2, i_3=i_4} \right) \quad (142)$$

and so:

$$\mathbb{E} \left[\|y^l\|^4 \right] = \frac{n_l c_4^l}{2} \sum_{i=1} \mathbb{E} \left[(y_i^{l-1})^4 \right] + \frac{6n_l}{n_{l-1}^2} \sum_{i_1 \neq i_2} \mathbb{E} \left[(y_{i_1}^{l-1})^2 (y_{i_2}^{l-1})^2 \right] \quad (143)$$

$$+ \frac{n_l(n_l-1)}{n_{l-1}^2} \sum_{i_1, i_2} \mathbb{E} \left[(y_{i_1}^{l-1})^2 (y_{i_2}^{l-1})^2 \right] \quad (144)$$

$$= \frac{n_l(c_4^l - 3(c_2^l)^2)}{2} \sum_i \mathbb{E} \left[(y_i^{l-1})^4 \right] + \frac{n_l(n_l+5)}{n_{l-1}^2} \mathbb{E} \left[\|y^{l-1}\|^4 \right] \quad (145)$$

$$= \frac{n_l \Delta}{n_{l-1}^2} \sum_i \mathbb{E} \left[(y_i^{l-1})^4 \right] + \frac{n_l(n_l+5)}{n_{l-1}^2} \mathbb{E} \left[\|y^{l-1}\|^4 \right] \quad (146)$$

For Gaussian distributions, $\Delta = 0$, proving the claim. \square

proposition 5. For a vanilla fully connected linear network, with intermediate outputs given by:

$$\forall 0 \leq l \leq L, y^l = \frac{1}{\sqrt{n_{l-1}}} W^{l\top} y^{l-1} \quad (147)$$

, where the weight matrices $W^l \in \mathbb{R}^{n_{l-1} \times n_l}$ are normally distributed, the following holds at initialization:

$$\mathbb{E}[\|y^l\|^2] = \frac{n_l}{n_{l-1}} \mathbb{E}[\|y^{l-1}\|^2] \quad (148)$$

$$\mathbb{E}[\|y^l\|^4] = \frac{n_l(n_l+2)}{n_{l-1}^2} \mathbb{E}[\|y^{l-1}\|^4] \quad (149)$$

Proof. The proof follows the derivation of Proposition 4 exactly, and will be omitted for brevity. \square

A.6. Proof of Theorem 5

In the following proof, for the sake of notation simplicity, we omit the notation k in $y_{(k)}^l$, and assume that y^l stands for the reduced network $y_{(k)}^l$. The recursive formula for the intermediate outputs of the reduced network are given by:

$$y^l = \begin{cases} y^{l-1} + y^{l-1, m} & 0 < l \leq L, l \neq k \\ y^{l-1, m} & l = k \end{cases} \quad (150)$$

where:

$$y^{l-1, h} = \begin{cases} \sqrt{\frac{\alpha}{n}} W^{l, k\top} q^{l-1, h-1} & 1 < h \leq m \\ \sqrt{\frac{\alpha}{n}} W^{l, h\top} y^{l-1} & h = 1 \end{cases} \quad (151)$$

with $q^{l-1, h} = \sqrt{2}\phi(y^{l-1, h})$.

We have for layer L using the results of Propositions 4 and 5:

$$\begin{aligned}
 \mathbb{E} [\|y^L\|^2] &= \mathbb{E} [\|y^{L-1}\|^2] + \frac{\alpha}{n} \mathbb{E} [y^{L-1, m-1 \top} W^{L, m} W^{L, m \top} y^{L-1, m-1}] \\
 &= \mathbb{E} [\|y^{L-1}\|^2] + \alpha \mathbb{E} [\|y^{L-1, m-1}\|^2] = \mathbb{E} [\|y^{L-1}\|^2] (1 + \alpha^m) \\
 &= \mathbb{E} [\|y^k\|^2] \prod_{l=k+1}^L (1 + \alpha^m) = \mathbb{E} [\|y^{k-1}\|^2] \prod_{l=k+1}^L (1 + \alpha^m) \alpha^m \\
 &= \prod_{l \neq k} (1 + \alpha^m) \alpha^m \mathbb{E} [\|y^0\|^4] = (1 + \alpha^m)^{L-1} \alpha^m \mathbb{E} [\|y^0\|^4] \quad (152)
 \end{aligned}$$

For the fourth moment, using the results of proposition 4 and 5, it holds:

$$\mathbb{E} [\|y^L\|^4] = \mathbb{E} [\|y^{L-1}\|^4] + \frac{\alpha^2}{n^2} \mathbb{E} [\|y^{L-1, m}\|^4] + 4 \frac{\alpha}{n} \mathbb{E} [(y^{L-1, m \top} y^{L-1})^2] + 2 \frac{\alpha}{n} \mathbb{E} [\|y^{L-1, m}\|^2 \|y^{L-1}\|^2] \quad (153)$$

We now handle each term separately:

$$\mathbb{E} [\|y^{L-1, m}\|^4] = \mathbb{E} [\mathbb{E} [\|y^{L-1, m}\|^4 | R^{L-1}]] \quad (154)$$

Using the results of Propositions 4 and 5:

$$\mathbb{E} [\|y^{L-1, m}\|^4 | R^{L-1}] = \alpha^{2m} (1 + \frac{2}{n}) (1 + \frac{5}{n})^{m-1} \|y^{L-1}\|^4 < \alpha^{2m} (1 + \frac{5}{n})^m \|y^{L-1}\|^4 \quad (155)$$

$$\mathbb{E} [(y^{L-1, m-1 \top} y^{L-1})^2] = \frac{\alpha}{n} \sum_{j_1 j_2 i_1 i_2} \mathbb{E} [y_{i_1}^{L-1, m-1} y_{i_2}^{L-1, m-1} y_{j_1}^{L-1} y_{j_2}^{L-1} w_{i_1, j_1}^{L, m} w_{i_2, j_2}^{L, m}] \quad (156)$$

$$= \frac{\alpha}{n} \mathbb{E} [\|y^{L-1, m-1}\|^2 \|y^{L-1}\|^2] = \frac{\alpha^m}{n} \mathbb{E} [\|y^{L-1}\|^4] \quad (157)$$

and:

$$\mathbb{E} [\|y^{L-1, m}\|^2 \|y^{L-1}\|^2] = \alpha^m \mathbb{E} [\|y^{L-1}\|^4] \quad (158)$$

Plugging it all into Eq. 153, and denoting:

$$\beta = 1 + 2\alpha^m (1 + \frac{2}{n}) + \alpha^{2m} (1 + \frac{5}{n})^m \quad (159)$$

$$(160)$$

we have after recursing through $l = L-1 \dots 1$:

$$\mathbb{E} [\|y^L\|^4] \sim \mathbb{E} [\|y^k\|^4] \beta^{L-k+1} \quad (161)$$

In the reduced architecture, the transformation from layer $k-1$ to layer k is given by an m layer fully connected network, with a linear layer on top, we can use the results from the vanilla case:

$$\mathbb{E} [\|y^L\|^4] \leq \alpha^{2m} (1 + \frac{5}{n})^m \beta^{L-1} \mathbb{E} [\|y^0\|^4] \quad (162)$$

Note that:

$$\beta \leq \left(1 + \alpha^m (1 + \frac{5}{n})^{\frac{m}{2}}\right)^2 \quad (163)$$

Denoting $\rho = (1 + \frac{5}{n})^{\frac{m}{2}}$, it holds for $\alpha < 1$:

$$Var(\|y^L\|^2 | y^0) \quad (164)$$

$$\leq \left(\alpha^{2m} \rho^2 (1 + \alpha^m \rho)^{2(L-1)} - \alpha^{2m} (1 + \alpha^m)^{2(L-1)} \right) \|y^0\|^4 \quad (165)$$

$$\alpha^{2m} (1 + \alpha^m)^{2(L-1)} (\rho^2 - 1) < Var(\|y^L\|^2 | y^0) < \alpha^{2m} (1 + \alpha^m \rho)^{2(L-1)} (\rho^2 - 1) \quad (166)$$

and so:

$$\alpha^{2m} \exp \left[\alpha^m (L-1) \right] (\rho^2 - 1) < Var(\|y^L\|^2 | y^0) < \alpha^{2m} \exp \left[2\alpha^m \rho (L-1) \right] (\rho^2 - 1) \quad (167)$$

Yielding:

$$Var(\left\| \frac{\partial f}{\partial W} \right\|^2) \sim \left(mL \sqrt{Var(f_{(k)})} \right)^2 \sim \mathcal{O} \left((mL)^2 \alpha^{2m} (\rho^2 - 1) \exp \left[2(L-1) \alpha^m \rho \right] \right) \quad (168)$$

A.7. Proof of Corollary 1

Proof. The proof is immediate using taylor expansion $\rho^2 - 1 \sim \frac{m}{n}$, and noticing that:

$$\lim_{L \rightarrow \infty} \exp \left[2(L-1) \alpha^m \rho \right] (mL)^2 \alpha^{2m} = \lim_{L \rightarrow \infty} \exp \left[\frac{2a(L-1)}{L} \right] \frac{(mLa)^2}{L^2} = \text{constant} \quad (169)$$

□

A.8. Proof of Theorem 6

In the following proof, for the sake of notation simplicity, we omit the notation k in $y_{(k)}^l$, and assume that y^l stands for the reduced network $y_{(k)}^l$. The recursive formula for the intermediate outputs of the reduced network are given by:

$$y^l = \begin{cases} \frac{1}{\sqrt{nl}} \sum_{h=k}^{l-1} W^{l,h\top} q^h & k < l \leq L \\ \frac{1}{\sqrt{nl}} \sum_{h=0}^{l-1} W^{l,h\top} q^h & 1 \leq l < k \\ \frac{1}{\sqrt{nk}} W^{k,k-1\top} q^{k-1} & l = k \end{cases} \quad (170)$$

with $q^h = \sqrt{2} \phi(y^h)$. We have:

$$\mu_L = \mathbb{E} \left[\|q^L\|^2 \right] = \frac{2}{Ln} \mathbb{E} \left[\left(\sum_{l=k}^{L-1} q^{l\top} W^{Ll} \right) Z^L \left(\sum_{l=k}^{L-1} q^{l\top} W^{Ll} \right) \right] = \frac{1}{L} \sum_{l=k}^{L-1} \mu_l \quad (171)$$

$$\begin{aligned} \mathbb{E} \left[\|q^L\|^4 \right] &= \frac{4}{n^2 L^2} \mathbb{E} \left[\left(\sum_{l=k}^{L-1} (q^{l\top} W^{Ll}) Z^L \sum_{l=k}^{L-1} (q^{l\top} W^{Ll}) \right)^2 \right] \\ &= \frac{4}{n^2 L^2} \mathbb{E} \left[\left(\sum_{l_1=k}^{L-1} (q^{l_1\top} W^{Ll_1}) Z^L \sum_{l_2=k}^{L-1} (q^{l_2\top} W^{Ll_2}) \sum_{l_3=k}^{L-1} (q^{l_3\top} W^{Ll_3}) Z^L \sum_{l_4=k}^{L-1} (q^{l_4\top} W^{Ll_4}) \right)^2 \right] \end{aligned} \quad (172)$$

Using the results from the vanilla architecture, and denoting $C_{l,l'} = \mathbb{E} \left[\|q^l\|^2 \|q^{l'}\|^2 \right]$, it then follows:

$$C_{L,L} = \frac{(n+5)}{nL^2} \sum_{l_1, l_2=k}^{L-1} C_{l_1, l_2} \quad (173)$$

From Eq. 173, it also holds that:

$$\sum_{l_1, l_2=k}^{L-2} C_{l_1, l_2} = \frac{n(L-1)^2}{n+5} C_{L-1, L-1} \quad (174)$$

It then follows:

$$\begin{aligned} \mathbb{E}(\|q^L\|^4) = C_{L, L} &= \frac{1}{L^2} \left(1 + \frac{5}{n}\right) \sum_{l_1, l_2=k}^{L-1} C_{l_1, l_2} = \frac{1}{L^2} \left(1 + \frac{5}{n}\right) \left(C_{L-1, L-1} + \sum_{l_1, l_2=k}^{L-2} C_{l_1, l_2} + 2 \sum_{l=k}^{L-2} C_{L-1, l} \right) \\ &= \frac{1}{L^2} \left(1 + \frac{5}{n}\right) \left(C_{L-1, L-1} + \frac{(L-1)^2 n}{a_{L-1}^2 (n+5)} C_{L-1, L-1} + 2 \sum_{l=k}^{L-2} C_{L-1, l} \right) \end{aligned} \quad (175)$$

$$(176)$$

The following also holds:

$$\forall l_1 > l_2 \geq k, \quad C_{l_1, l_2} = \mathbb{E} \left[\left(\sum_{l=k}^{l_1-1} q^{l\top} W^{l_1, l} Z^{l_1} \right)^2 \|q^{l_2}\|^2 \right] = \frac{1}{l_1} \sum_{l=k}^{l_1-1} C_{l, l_2} \quad (177)$$

and so:

$$C_{L, L} = \frac{(n+5)}{nL^2} \left(C_{L-1, L-1} + \frac{(L-1)^2 n}{1(n+5)} C_{L-1, L-1} + \frac{2}{L-1} \sum_{l_1=k}^{L-2} \sum_{l_2=k}^{L-2} C_{l_1, l_2} \right) \quad (178)$$

$$= \frac{(n+5)}{nL^2} \left(C_{L-1, L-1} + \frac{(L-1)^2 n}{(n+5)} C_{L-1, L-1} + \frac{2n(L-1)}{(n+5)} C_{L-1, L-1} \right) \quad (179)$$

$$= \frac{(n+5)}{nL^2} C_{L-1, L-1} \left(1 + \frac{(L-1)^2 n}{(n+5)} + \frac{2n(L-1)}{(n+5)} \right) \quad (180)$$

$$= C_{L-1, L-1} \left(\left(\frac{1}{L} + \frac{(L-1)}{L} \right)^2 + \frac{5}{nL^2} \right) = C_{L-1, L-1} \left(1 + \frac{5}{nL^2} \right) \quad (181)$$

Telescoping through $l = L-1 \dots k+1$:

$$C_{L, L} = C_{k+1, k+1} \prod_{l=k+2}^L \left(1 + \frac{5}{nl^2} \right) \quad (182)$$

For the reduced architecture, the transition from q^k to q^{k+1} is a vanilla ReLU block, and so using the result from the vanilla architecture:

$$C_{L, L} = C_{k, k} \prod_{l=k+2}^L \left(1 + \frac{5}{nl^2} \right) \frac{n+5}{n(k+1)^2} = C_{0, 0} \prod_{l \neq k+1} \left(1 + \frac{5}{nl^2} \right) \frac{n+5}{n(k+1)^2} \quad (183)$$

Telescoping the mean:

$$\mu_L = \frac{1}{L} \sum_{l=k}^{L-1} \mu_l = \frac{\mu_{L-1}}{L} + \frac{L-1}{L} \mu_{L-1} = \mu_{L-1} = \mu_{k+1} = \frac{1}{k+1} \mu_k = \frac{1}{k+1} \mu_0 \quad (184)$$

It then follows:

$$Var(\|q^L\|^2 | q^0) = C_{L, L} - \mu_L^2 = \|q^0\|^4 \left(\prod_{l \neq k+1} \left(1 + \frac{5}{nl^2} \right) \frac{n+5}{n(k+1)^2} - \frac{1}{(k+1)^2} \right) \quad (185)$$

$$= \frac{\|q^0\|^4}{(k+1)^2} \left(\prod_{l \neq k+1} \left(1 + \frac{5}{nl^2} \right) \frac{n+5}{n} - 1 \right) \leq \frac{\|q^0\|^4}{(k+1)^2} \left(\exp \left[\sum_{l=1}^L \frac{5}{nl^2} \right] - 1 \right) \sim \mathcal{O} \left(\frac{e^{\frac{5}{n}} - 1}{k^2} \right) \quad (186)$$

Yielding:

$$Var(\|\frac{\partial f}{\partial W}\|^2) \leq \left(\sum_{k=1}^L \sqrt{Var(f_{(k)})} \right)^2 \sim \mathcal{O}\left((e^{\frac{5}{n}} - 1)(\sum_{k=1}^L \frac{1}{k})^2\right) = \mathcal{O}\left((e^{\frac{5}{n}} - 1) \log(L)^2\right) \quad (187)$$

A.9. Proof of Corollary 2

Proof. The proof is immediate using taylor expansion $(e^{\frac{5}{n}} - 1) \sim \frac{5}{n} + \mathcal{O}(\frac{1}{n^2})$. \square